Report T14 / R23

Reactive Transport for Fuel Containing Materials

(Dynamical Compartment Model)

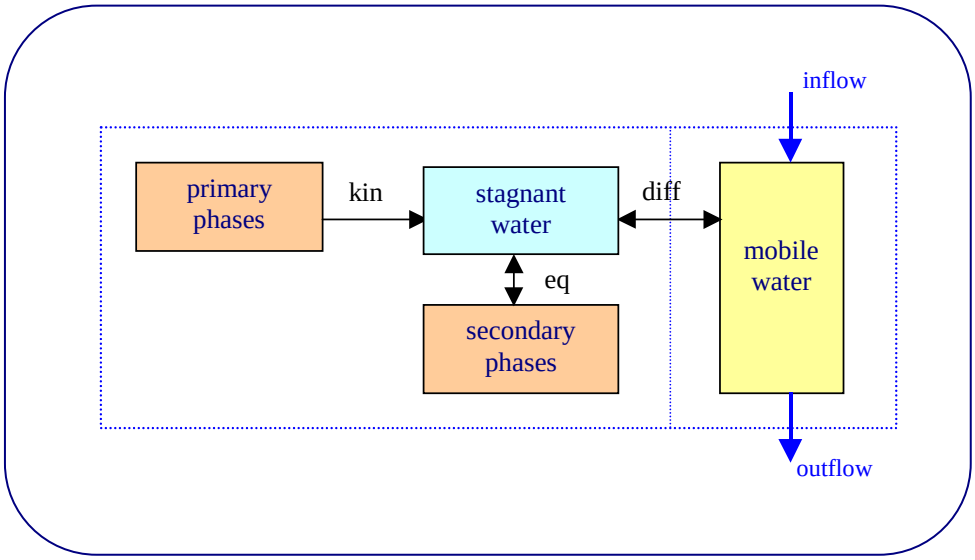

to

Chernobyl NPP Unit 4 – SIP EBP Package "D"

submitted by

UIT GmbH Dresden, Germany

September 2000

Report to

Chernobyl NPP Unit 4 – SIP EBP Package “D”

Task 14 / R23
(Predicted Data Changes)

Reactive Transport for Fuel Containing Materials

– Dynamical Compartment Model –

H. KALKA

September 2000

Contents

1 Introduction

1.1 Objectives and Background

Objectives. This report presents a model concept for the *dynamical* description of the *chemical weathering* of fuel containing materials (FCM), construction materials (CM), and dumping materials (DM) due to the influence of water and atmosphere. To simulate the migration of uranium in aqueous form and its redistribution in the Shelter the model combines mass transport with reactions including both equilibrium processes (thermodynamics) and kinetics.

Based on the conceptual model this report includes the mathematical derivation of the main equations and identifies the input data as well as the most influencing parameters for a straightforward calculation. The route from the conceptual model to the numerical model described in this report is as follows:

Conceptual Model

⇓ *quantification*

Mathematical Model

⇓ s*patial and temporal discretization*

Numerical Model (code `dynFCM`)

After model construction and model calibration the compartment model becomes a tool for forecast and for dynamical simulation of different leaching scenarios within the Chernobyl Shelter. In this way the reactive transport model is useful to (see Fig. 1):

- evaluate the time-dependent FCM distribution and evolution history,
- develop Shelter water management strategy (remedial alternatives),
- organize a large volume of field data,
- provide guidance for additional data collection.

In case of application of active leaching technologies for FCM removal (see T20/D1-report and its appendix) this model could be useful for selecting optimized removal strategies and for the interpretation of the demonstration (pilot) experiments.

Generalized Modeling Approach. A variety of tasks are required in construction of a dynamical Shelter model. The main steps include:

- the development of a conceptual model (Chapter 2),
- the creation of the mathematical model (Chapter 3),
- the definition of the input data structure and specification of the model parameters,
- its realization as a software package `dynFCM` for Windows-based personal computers,
- model calibration and validation testing by execution of various trials.

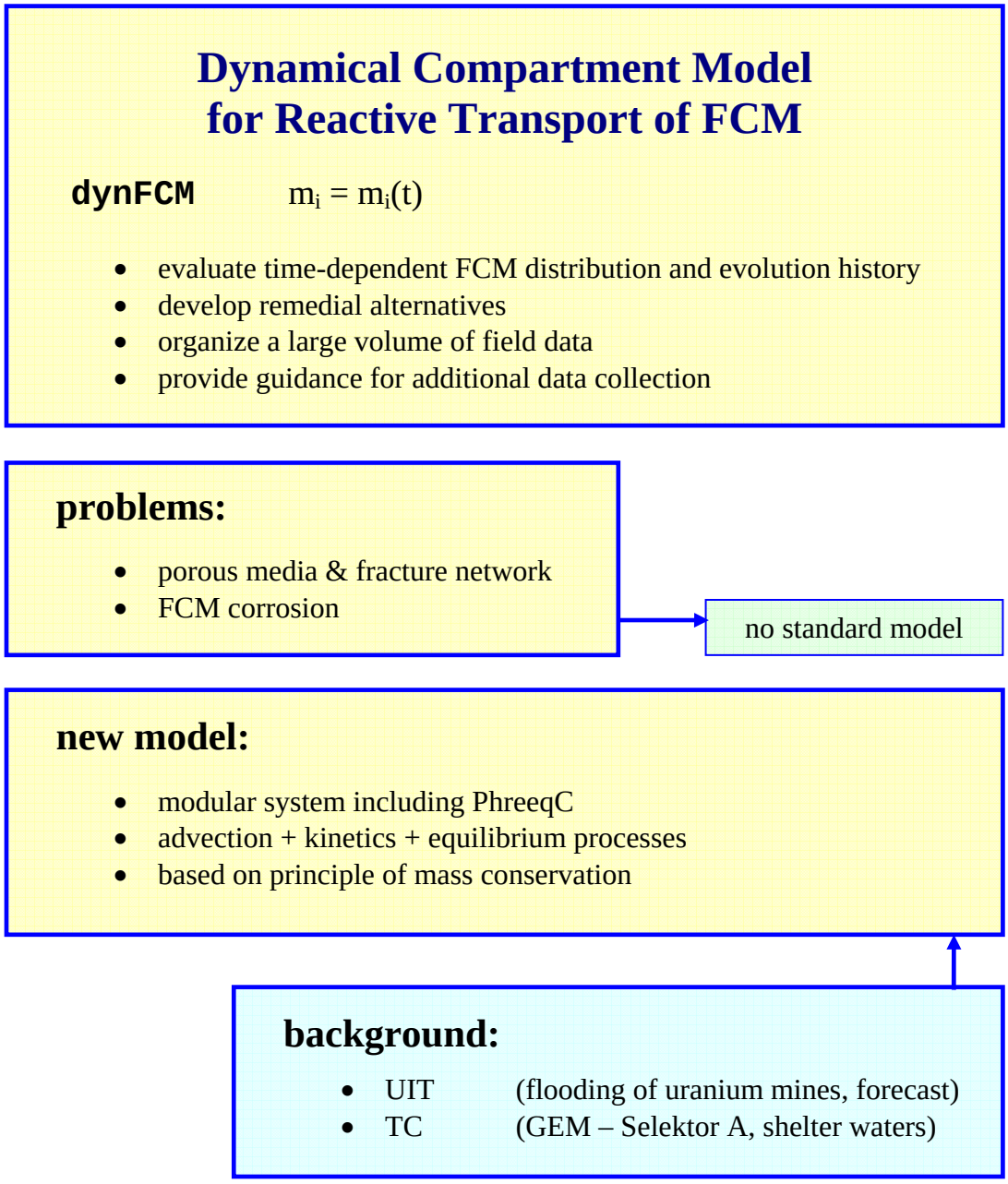

Fig. 1 Objectives, problems and background of the dynamical compartment model (dynFCM)

Once a model is successfully calibrated, it can be used predictively. Many effort was done for the conceptual model. To avoid overkill in the complexity and numerics the model which bases on the principle of local and global mass balance should be as simple as possible. Therefore, in the first stage of modeling only the dominant processes will be included whereas second-order processes are synthesized into “effective” or macroscopic parameters. In a second step then the effective parameters will be approached by “microscopic” models or theories. For example:

1st stage: main processes (FCM-water system and CM-water-system) and main elements (Na, K, Ca, Mg, Cl, S, C, H, O, Fe, Al, U),

2nd stage: "second-order processes" (Zr-U-O phases, etc.) and complete element spectrum including all radionuclides,

[3rd stage: LFCM destruction and dust production (hot particles) including aerosol-transport within the shelter.]

The present report describes all procedures and parameters to realize the 1st stage.

Background. For the numerical treatment of the advection-reaction processes within the highly complex and heterogeneous system "Shelter" there is *no* standard model or software package available. The well-known code families for transport and reactive transport [DS98] are not adequate tools to describe the processes within the Shelter because of the complicated – and in most cases unknown – combinations of flow through porous media *and* through fracture networks. Therefore a new dynamical approach for an "average" or "effective" description of the problem is appropriate.

For this reason – based on existing experiences, observed data, and software tools – a Shelter-specific dynamical model for reactive transport of FCM will be developed. The main experiences are:

First. In the last years UIT has developed a special software package for the consistent simulation of the hydrological and geochemical conditions in great heterogeneous and complex systems (flooding of Uranium mines in Saxonia, Thuringia, Colorado; long-term forecast, kinetic oxidation processes, etc.) [Ka98, Pau98, UIT00, and about 15 internal reports] which includes the chemical code PhreeqC [Par95] as a special subroutine to calculate the (equilibrium) processes. The kinetics for dissolution / precipitation and other non-equilibrium processes are treated separately in time steps of size Δt.

Second. Since 1991 at Technocentre in Kiev thermodynamic evaluation and studies of the interaction of Shelter waters with FCM and CM based on a convex programming approach to Gibbs free energy minimization (Selektor-A code) are performed [Sin97, Sin98, Ku98]. These investigations establish the stabile phases as well as the appropriate equilibrium constants (log-k values) which are necessary for equilibrium calculations with PhreeqC.

Finally, all available information's from other SIP documents are used: Task 10 [T10], Task 13 [T13], and Task 14 [T14].

Modular software design. The model `dynFCM` will be build with a modular design that consists of a main program and "packages". The packages – most of them already exist – are groups of independent subroutines that carry out specific simulation tasks such as transport, kinetics, diffusion, equilibrium calculations with PhreeqC etc. This modular design is useful in several ways. It provides a logical basis for organizing the actual code with similar program elements or functions grouped together. Such a structure facilitates the integration of new packages to enhance the code's capabilities.

The software is written in the object oriented programming language C++ which goes along with the ideas of modular design [St94].

1.2 List of Abbreviations, Terms and Symbols

1.2.1 List of Abbreviations

CF Core Fragments
CM Construction Materials (concrete, steel)
CSH Amorphous Calcium Silicate Hydrogel Phase
DM Materials dumped by helicopters to smoother the reactor fire during the "Active phase Accident Management Actions" (Na_3PO_4, dolomite, ...)
FCM Fuel Containing Materials
HP Hot Particles
IAP Ion Activation Product
LFCM Lava-like Fuel Containing Materials
NIAS Nuclear Island Auxiliary System
SUM Secondary Uranium Minerals
TST Transition-State Theory

Computer Codes

dynFCM software package of the Dynamical Compartment Model for Reactive Transport of FCM within the Shelter (the object of this report)
PhreeqC Program for Geochemical Calculations from U.S. Geological Survey [Par95, PA99]
Selektor-A Convex programming approach to Gibbs Free Energy Minimization, Technocentre Kiev

Physical Units:

	L	length (m)
	T	time (s)
	M	mass (kg or mol)

[Note that the abbreviation for the length L and the abbreviation for the volume unit *liter* (L) is the same, 1 L = 1 dm^3. The actual meaning becomes clear from context.]

The molar concentrations of chemical species are also symbolized by brackets: [H_2O], [U], etc.

1.2.2 List of Mathematical Symbols

To give a mathematical foundation of the model a lot of symbols should be defined. The subscripts i and j refer to the compartment i and j. So-called *global* quantities are independent of i and/or j. In general, all concentrations c and masses m are vectors of K species (for example: $c_i^{(k)}$ denotes the concentration of species k in compartment i, with $1 \le k \le K$). However, to keep the notation as simple as possible the superscripts k will be dropped.

a	thickness of the stationary layer	L
A_i	base area of compartment i	L^2
A_i^D	surface of “diffusion layer”	L^2
A_i^S	(initial) surface area of the solid which is in water contact	L^2
A_s	$= A_i^S / m_i^s$, specific surface area (in m^2/g)	L^2M^{-1}
c_i	concentration in the *mobile* aqueous phase	ML^{-3}
$\tilde{c}_i$	concentration in the *stagnant* aqueous phase	ML^{-3}
c^{eq}	concentration in equilibrium with solid phase	ML^{-3}
c^0	pure water concentration (H_2O = 55.5 mol/l)	ML^{-3}
c_0	concentration of external inflow water (pristine water)	ML^{-3}
D	diffusion coefficient	L^2T^{-1}
Eh	redox potential	mV
f_{ij}	hydraulic mixing factors between compartment i and j	1
H_i	height of compartment i	L
k	thermodynamic equilibrium constant	
k_{ij}	splitting factor for flow paths between compartment i and j	1
i	compartment number (or label)	$0 \le i \le N$
$m_i^{aq} = c_i V_i$	element mass in the *mobile* aqueous phase (bulk water)	M
$\tilde{m}_i^{aq} = \tilde{c}_i \tilde{V}_i$	element mass in the *stagnant* aqueous phase (pore water)	M
m_i^s	element mass in the solid phase	M
m_i^{s1}	element mass in the solid phase of primary mineral	M
m_i^{s2}	element mass in the solid phase of secondary mineral	M
n	porosity	L^3/L^3
N	total number of compartments	1
Q^{ingr}	water ingress to the Shelter	L^3T^{-1}
Q^{egr}	water egress from the Shelter	L^3T^{-1}
$Q_{i\to j}$	hydraulic flow rate from compartment i to compartment j	L^3T^{-1}
$Q_i^{ext\ in}$	external inflow rate to compartment i	L^3T^{-1}
$Q_i^{ext\ out}$	external outflow rate from compartment i	L^3T^{-1}
$Q_i^{int\ in}$	internal inflow rate to compartment i	L^3T^{-1}
$Q_i^{int\ out}$	internal outflow rate from compartment i	L^3T^{-1}
Q_i^{in}	external plus internal inflow rate to compartment i	L^3T^{-1}
Q_i^{out}	external plus internal outflow rate from compartment i	L^3T^{-1}
Q_i^{cnd}	condensation rate in compartment i	L^3T^{-1}
Q_i^{evp}	evaporation rate in compartment i	L^3T^{-1}
r	specific rate for dissolution	$ML^{-2}T^{-1}$
R_i	source term rate for compartment i	$ML^{-3}T^{-1}$
R_i^D	diffusion rate	$ML^{-3}T^{-1}$
R_i^S	overall reaction rate for dissolution	$ML^{-3}T^{-1}$

V_i	volume of mobile water (bulk water) in compartment i	L^3
$\tilde{V}_i$	volume of stagnant water (pore water) in compartment i	L^3
V_i^R	reaction volume	L^3
V_i^S	"reactive" water volume in contact with the solid	L^3
V_i^D	volume of "diffusion layer" (between stagnant and mobile water)	L^3
z_i	bottom elevation of compartment i (above sea level)	L
$\delta(t)$	Dirac's delta-function	T^{-1}
$\Theta(x)$	Heaviside step-function	1
θ	volumetric water content ($\leq$ porosity n)	L^3/L^3
ρ_s	bulk density of the solid	ML^{-3}
κ	parameter for first-order kinetics	T^{-1}

2 Conceptual Model

The compartment model is based on a coarse spatial discretization of the model space (system of compartments) and fine temporal discretization (Δt in order of hours). Since there is no complete information about the transport and reaction processes on a "microscopic" scale the compartment model describes the processes in an average manner using effective parameters which will be adjusted to observed data (model calibration). This Chapter contains the model concept; the mathematical model which is based on the principle of mass conservation will be derived in Chapter 3.

2.1 Basic Idea

The model space "Shelter" is divided into N compartments or regions (see Fig. 2). The compartments are coupled by hydraulic flows (*internal* couplings between an arbitrary number of other compartments and *external* couplings between a compartment and the outside). In contrast to the 3D hydrogeology models which are based on a fine-size grid of cells the compartment model is quasi-3D.

[Here the term *compartment* rather than *cell* is used to distinguish the present model from transport models used in geohydrology which are based on grid structures. Synonyms for compartment are box, region or domain.]

2.1.1 Dual-Zone Structure of a Compartment

To describe reactive transport phenomena each compartment is conceptualized as consisting of two distinctive zones (see also Fig. 4):

transport zone T:	for the mobile phases	(mobile water, gas),
reaction zone R:	for the immobile phases	(stagnant water, solids, surfaces).

Zone T is responsible for the transport (advection), i. e., the mass transfer between neighbor compartments and from/to the outside of shelter. In the reaction zone R the interaction be-

tween stagnant water (pore solutions) and solid phases takes place. Both zones are connected by mass transfer due to diffusion between stagnant water and mobile water.

[The stagnant water should not be confused with the water pools in the rooms inside the Shelter. In this context stagnant water signifies the *pore* water or the thin water film surrounding the solid phases – see Fig. 3. On the other hand, the water pools contain excess water which belongs in the present notation to the mobile water phase or so-called bulk water and which volume is in general time-dependent.]

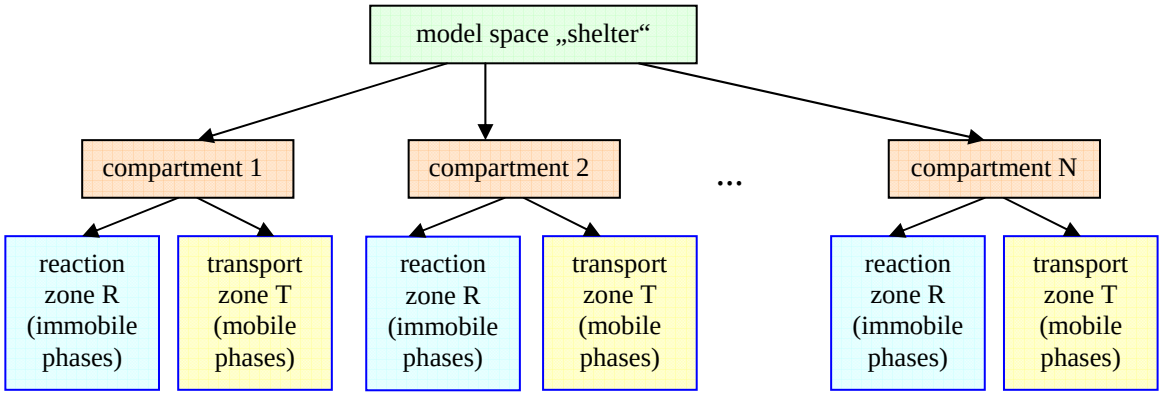

Fig. 2 Decomposition of the model space “Shelter” into N compartments

To illustrate the dual-zone concept, Fig. 3 shows a piece of porous media. The interconnected and sufficiently large pore spaces form preferential flow pathways for *mobile* waters while dead-end and small pore spaces are filled with *immobile* waters. The immobile water is in direct contact with the solid matrix and causes its dissolution. The increased concentration in the immobile water phase then gives rise to the diffusion of solutes into the mobile water phase.

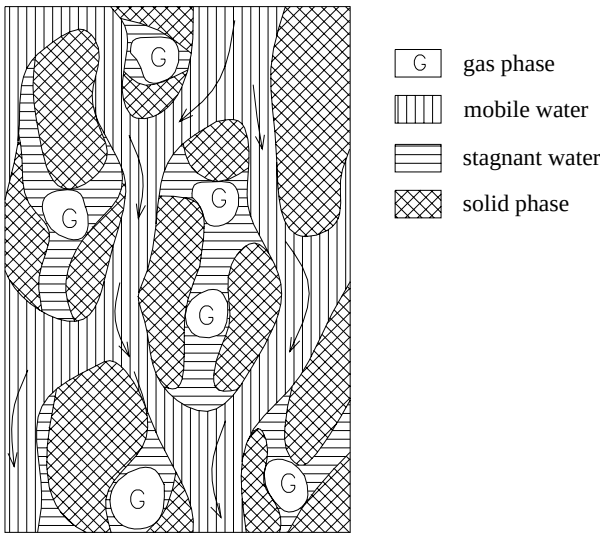

Fig. 3 Mobile and immobile phases in a piece of porous media

The lower part of Fig. 4 shows the following processes more abstractly: First, the kinetic dissolution of a primary phase is treated as

a surface controlled two-step process (here two parallel dissolution paths are considered such as discussed in [Ca94], respectively) which increases the concentrations in the pore solution. The pore solution – that is the stagnant water phase – is assumed to be in equilibrium with secondary mineral phases which allows precipitation as a rate limiting process. Due to diffusion there is a mass exchange between both the stagnant and mobile water phases. Finally, the advection in the mobile water phase transports the mass to other compartments and/or to the environment.

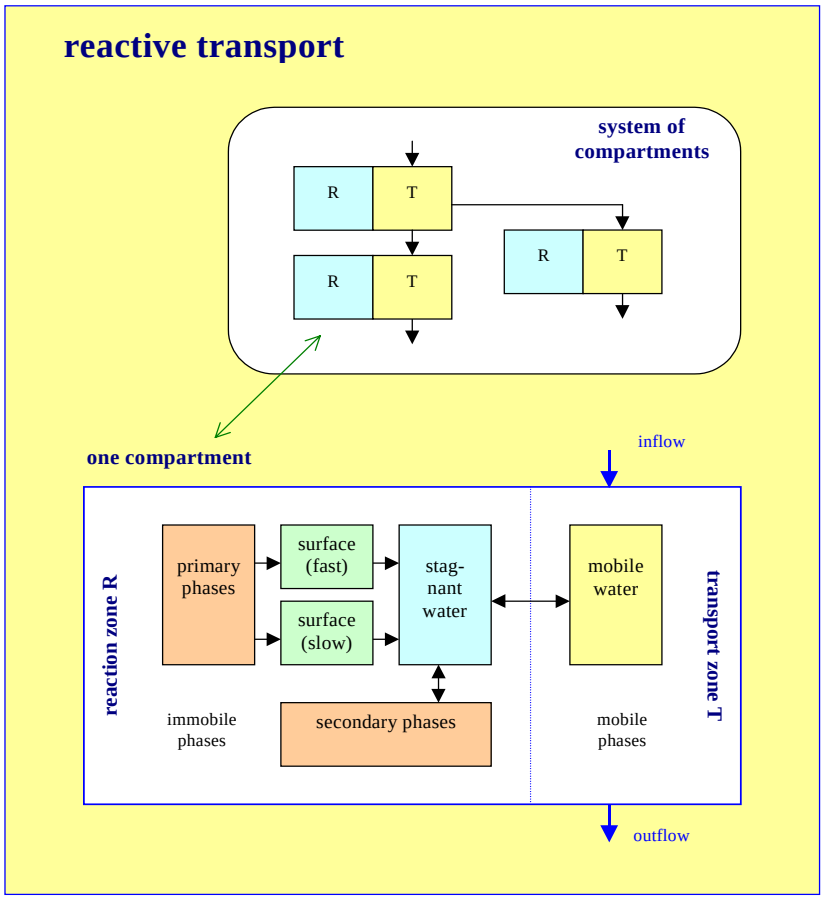

Fig. 4 Example for a small complex of compartments and the internal structure of one compartment

[*Model of surface-controlled dissolution:* The kinetics of surface-controlled dissolution is treated as a two-step process. The first step involves a rapid, reversible sorption of reactive chemical species (protons, ligands, reductans) from solution onto the surface. The second step results in detachment of a metal from the surface of the crystalline lattice. The rate law for surface-controlled dissolutions is based on the assumption that the first step is fast and the second step rate-limiting. Rapid regeneration of the surface and reequilibration of the reactive surface species is assumed.]

The aim is now to apply and modify this model framework to the special case of the Chernobyl Shelter. Therefore, in the subsequent Sections and Chapters the main mechanisms and transformation steps will be defined. For the first model version there are at least two main assumptions:

- The dissolution of both the fuel containing materials (FCM) and the construction materials (CM) occurs separately within each compartment and each time step Δt (see Fig. 5). In other words, the mobile water gets subsequently contact with stagnant water in cement pores and stagnant water in fuel pores. (The same holds also for the dumping materials if they are present in the compartment.)
- Due to the lack of data for the complicated UO_2 dissolution process which is influenced by the radiolysis of water the surface-controlled two-step mechanism will be treated as a *single*-step process using an effective rate r_{eff}. The value of the effective rate will be determined by adjustment to measured data and water compositions (model calibration).

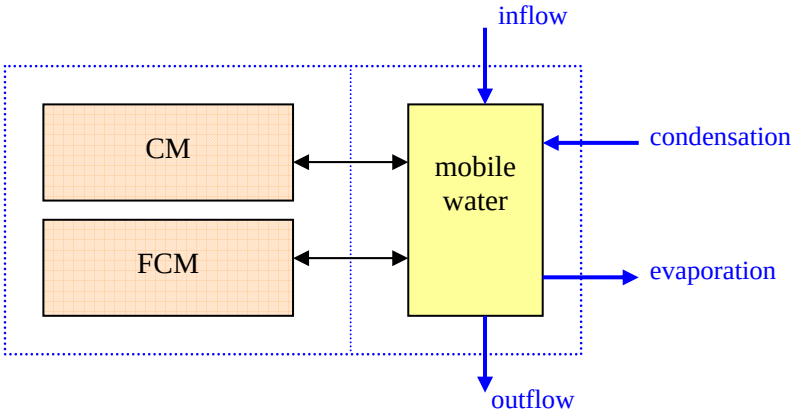

Fig. 5 Scheme of the solid-aqueous-interaction in one compartment containing the subsystems FCM and CM

As shown in Fig. 5 the sequence of interactions is chosen in such a way, that at first the water gets contact to the cement which enhance both the pH-value and the alkalinity and only afterwards the water with its special composition enters the FCM regions. These processes take place in every compartment which gives rise for a gradual increasing in the water concentrations of all solutes when water percolates through the Shelter as a system of compartments (principle of superposition).

A more detailed description of the reactive processes is given *qualitatively* in Sec. 2.3 and *mathematically* in Sec. 3.4.1.

2.1.2 Types of Fuel Containing Masses

The FCM is distributed over different types of masses:

(1) $$m_i^{FCM}(t) = m_i^{CF} + m_i^{LFCM} + m_i^{HP} + m_i^{SUM} + m_i^{sol}$$

where for each compartment i there is

m_i^{CF} unaltered nuclear fuel in UO_2 form (core fragments – CF),

m_i^{LFCM} lava-type fuel containing material (LFCM),

m_i^{HP}	dispersed fuel in form of "hot particles" up to 10 – 40 μm (HP),
m_i^{SUM}	secondary uranium minerals,
$m_i^{sol} = m_i^{aq} + \tilde{m}_i^{aq}$	FCM in solutions (mobile plus stagnant aqueous phases).

Here, the aqueous phase is decomposed into a *stagnant* phase (thin film surrounding the materials, pore solutions) and a *mobile* phase (water which transports solutes within the Shelter, initially pristine or rain water). In this way, the first four terms in Eq. (1) represent the *immobile* inventory, whereas only the last term includes the *mobile* inventory in form of the mobile aqueous phase.

The lava (LFCM) is a result of high temperature interaction of nuclear fuel with structures of the reactor block (backfilling materials: clay, sand, dolomite, boron, carbide, lead). The matrix of LFCM is a silicat glass (> 65 wt. % of SiO_2) containing K, Ca, Mg, Al, U, Zr impurities with no more than 3 – 4 % of each element.

The composition of HP varies according to the percentage of UO_{2+x} and different components of the structural minerals (Fe, Zr, Si etc.) up to the pure UO_2. Additionally, there are different oxidation states of UO_2, that is $x < 0$.

Whereas CF, LFCM and HP are so-called *primary* phases the SUM represents the *secondary* phases. As time evolves mass from the primary phases dissolutes and will be accumulated in both secondary minerals (SUM) and solutions; the outflow to the environment proceeds then via the solution transport.

The mass distribution in Eq. (1) is time dependent due to corrosion and alteration processes. In general there are various physico-chemical transformation paths for FCM:

- unaltered fuel (CF) corrosion path,
- LFCM corrosion path,
- HP dissolution,
- evaporation path,
- dust production.

2.1.3 Other Mass Types (Primary Phases)

To simulate the origin and the history of Shelter waters it is necessary to consider the interactions with construction materials (CM) such as concrete and with the material dumped from helicopters (DM): for example 2 500 t trinatriphosfatum Na_3PO_4 and 800 t dolomite [Sich94]. Thus, trinatriphosfatum enhances the Na and PO_4 content in the Shelter water.

The interaction of pristine water with concrete generates an alkaline and carbonate solution with a relatively law redox potential of Eh ≈ -100 mV.

2.2 Compartment Structure of "Chernobyl Shelter"

In this Section the main geometric data (Sec. 2.2.1) and hydraulic data (Secs. 2.2.2 and 2.2.4) for the compartment model are defined.

2.2.1 Geometrical Structure

The model space "Chernobyl Shelter" is subdivided into 18 compartments which are hydraulically coupled by a uniform flow field (see Fig. 6). The main characteristics of the compartments regarding the geometry and material are listed in Tab. 1. It contains the abbreviation and names of compartments, FCM masses (CF, LFCM, HP) in kg, the amount of solution in water pools in m^3, the amount of *concrete* in m^3 as a type of CM, as well as the geometrical parameters: bottom elevation z_i above sea level [m], height H_i [m] and base area A_i [m^2].

According to Tab. 1 the following mass balance is obtained:

CF	56.5 t
LFCM	115.0 t
HP	10.0 t
CF (outside Shelter: Pioneer Wall)	3.0 t
CF (outside Shelter: Fuel Channel from CH)	5.5 t
total FCM:	190.0 t

The masses of CF which are outside the Shelter (Pioneer wall, Fuel Channel from CH) are not included in the model space.

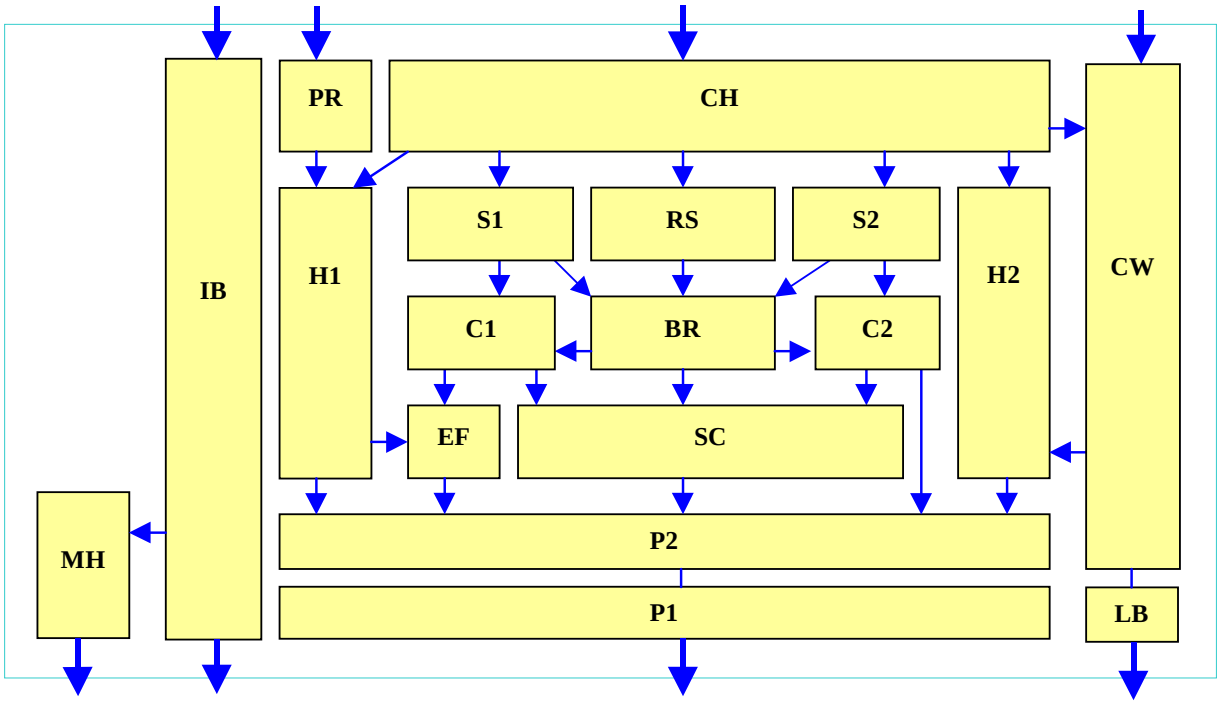

Fig. 6 Compartment structure of the model space „Chernobyl Shelter"

The total amount of concrete is 58 670 m^3; its average density is about $\rho = 2.3$ g/cm^3. (Additional materials not included in Tab. 1 are: (a) in compartment CH the minerals dolomite, kaliymetaborat and (b) in compartment BR the mineral serpentinite.)

The distribution of the dumping material trinatriphosfatum (Na_3PO_4) with a total amount of 2 500 t mass [Sich94] is as follows: 85 % in CH, 5 % in RS, and each of PR, H1, H2, S1, S2 with 2 %.

Volumes of water in *stagnant* pools are about 400 m^3 and these have been stable during recent years. The major water accumulations are in compartments which are lower than level 12.5 m. During snow-melt and high rainfall small *temporary* pools are generated at upper levels [T13].

Tab. 1 Compartments of the model space „Shelter“

	Compartment	FCM				CM	Bottom Elongation [m]	Height [m]	Base Area [m^2]
		CF [kg]	LFCM [kg]	HP [kg]	Soln [m^3]	Concrete [m^3]			
CH	Central Hall	29000		2500		1000	31.00	28.80	1980
RS	Reactor Shaft	20000	16000	600		200	14.20	17.30	520
S1	Side Box 1			300		150	13.80	19.00	380
S2	Side Box 2			300		150	13.80	19.00	380
PR	Pump Room			360		100	12.50	48.00	520
BR	Below Reactor Room	6000	53000	500	2	200	10.00	2.25	300
C2	Corridor 2			400	4	250	9.70	3.50	350
C1	Corridor 1		11000	400	4	250	9.30	3.50	300
SC	Steam Corridor		25000	500	6	800	6.00	2.00	864
EF	Elephant’s Foot (217/2)		500	100	4	70	6.00	3.00	246
H1	High Density Box 1			230		100	5.00	26.50	260
H2	High Density Box 2			230		100	5.00	26.50	260
P2	Steam Condens. Pool 2		8000	200	60	500	2.20	3.20	1728
P1	Steam Condens. Pool 1		1500	160	50	400	-0.65	2.35	1728
CW	Cascade Wall	1500		1900		54000	-1.30	42.50	700
LB	Low Level Box			140	270	200	-2.35	3.00	300
IB	Intermediate Building			880		200	-4.60	59.60	780
MH	Machine Hall			300			-4.60	35.00	6000

Since the base area A_i in Tab. 1 refers to the flow field (cross section and/or projections) it differs in some cases to the *real* area of the rooms and constructions (see for example Cascade Wall).

2.2.2 External Water Flow

As shown in Fig. 6 the flow field separates the model space into two parts which are disconnected: (a) the main part consisting of Unit “B” including parts of NIAS, and (b) the Machine Hall MH with the Intermediate Building IB. The purpose of this Section is to apply the Water Balance Assessment from Task 13 [T13] to the compartment model (here only for the main part, that is, Unit “B” and parts of NIAS).

In general the water ingress Q^{ingr} and the water egress Q^{egr} are time-dependent due to seasonal fluctuations, so that the water balance will be given for a given period of, say, one year:

(2) water balance: $$\int_0^{1\,year} Q^{ingr}(t)\,dt = \int_0^{1\,year} Q^{egr}(t)\,dt,$$

which reflects the fact that the ingress water volume and the egress water volume should be equal. In this way the general case is considered, where during shorter periods excess water can be accumulated inside the Shelter (change in water storage).

There are at least three *sources* of water ingress: the precipitation (rainfall, snow-melt) with average rate Q^{pp}, the liquids for dust suppression with rate Q^{ds}, and the condensation with rate Q^{cnd}. All rates are in units L^3/T (for example m^3/a or L/h). Removal of water from the Shelter (water egress) involves the leakage to surrounding structures (including pumping) with rate $Q^{ext\,out}$ and the evaporation with rate Q^{evp}. Thus we have:

(3) water ingress: $Q^{ingr}(t) = Q^{ext\,in} + Q^{cnd}$ with $Q^{ext\,in} = Q^{pp} + Q^{ds}$

(4) water egress: $Q^{egr}(t) = Q^{ext\,out} + Q^{evp}$.

The following upper limit of average water ingress is given in [T13]:

precipitation Q^{pp}	1 870 m^3/a
dust suppressing liquids Q^{ds}	270 m^3/a
condensation Q^{cnd}	1 650 m^3/a
net water ingress Q^{ingr}	3 790 m^3/a

This value is in annual balance with the average water egress:

leakage to surrounding structures $Q^{ext\,out}$	1 690 m^3/a
evaporation Q^{cnd}	2 100 m^3/a
net water egress Q^{egr}	3 790 m^3/a

Both the water ingress and the water egress define the time-dependent “boundary conditions” to calculate the internal flow field inside the Shelter (see Sec. 3.1.2). For this reason the global Shelter-quantities given above must be “redistributed” over all compartments i in the following manner:

(5) $$Q^{ext\,in} \Rightarrow Q_i^{ext\,in} \quad \text{with} \quad Q^{ext\,in} = \sum_i Q_i^{ext\,in},$$

(6) $$Q^{ext\,out} \Rightarrow Q_i^{ext\,out} \quad \text{with} \quad Q^{ext\,out} = \sum_i Q_i^{ext\,out}.$$

This should be done for all types of flow rates. Thus, for the condensation and evaporation rates the following estimate will be done:

(7) $$Q_i^{cnd} = \alpha_i Q^{cnd} \quad \text{and} \quad Q_i^{evp} = \alpha_i Q^{evp}$$

with the volume ratio:

(8) $$\alpha_i = \frac{A_i H_i}{\sum_i A_i H_i}.$$

Note that in the above sum are not included the two compartments MH and IB.

The external rates $Q_i^{ext\ in}$ and $Q_i^{ext\ out}$ are shown in Tab. 2 in units L/h (1 m^3/a = 0.114 L/h). In Tab. 2 only the few compartments are listed which are external water sources or sinks; their net flows fit the annual rates given above. According to Eq. (3) the external inflow rate is the sum of both precipitation and the amount of liquids for dust suppression (

Tab. 2 External inflow and outflow rates [L/h] using as "boundary conditions"

compartment	Q_i^{pp} [L/h]	Q_i^{ds} [L/h]	$Q_i^{ext\ in}$ [L/h]	$Q_i^{ext\ out}$ [L/h]
CH	132.1	30.8	162.9	
PR	34.7		34.7	
CW	46.7		46.7	
P1				151.0
LB				41.9
total	213.5	30.8	244.3	192.9

In Tab. 2 are not included the external flow rates of the compartments MH and IB. The corresponding quantities are estimated:

Machine Hall (MH): $Q_i^{ext\ in} = 0$ $Q_i^{ext\ out} = 30$ L/h

Intermediate Building (IB): $Q_i^{ext\ in} = 48$ L/h $Q_i^{ext\ out} = 18$ L/h.

2.2.3 Condensation and Evaporation

Within a so-called "two-period model" seasonal fluctuations of the flow field can be simulated by using time dependent evaporation and condensation rates (see Fig. 7). Condensation occurs during the period May-August (4 month) when moisture content and temperature of the air entering the Shelter is greater than that of the structures inside the Shelter so that as a result moisture vapor condenses from the incoming air. Otherwise, evaporation occurs mainly during the period September-April (8 month) when dry air enters the Shelter rooms.

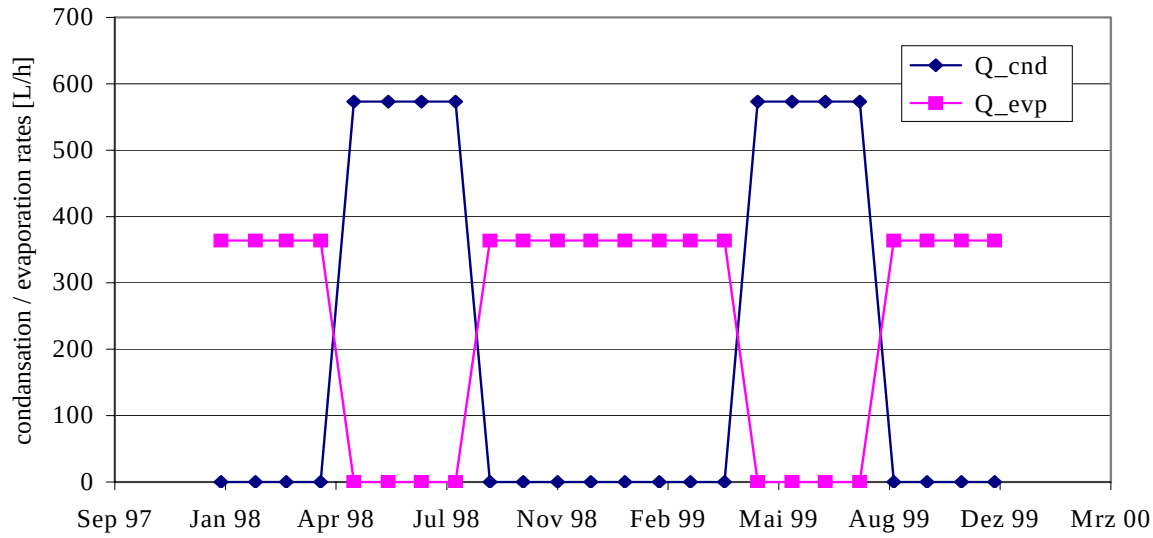

Fig. 7 Example for the time-dependence of the condensation and evaporation rates (seasonal fluctuations)

2.2.4 Internal Water Flow

The water flow through adjacent compartments represents the internal flow field. Its time-dependence is determined by the "boundary conditions": the external flow rates including condensation and evaporation. In principle there are two ways for using these "boundary conditions" to calculate the internal flow field:

Case 1: The external inflow rate will be given (not outflow rates). The model determines the time-dependent $Q_i^{ext\ out}$ under the condition that the water volume inside all compartments is zero or constant, $V_i(t) = const$ (no change in water storage). The time-dependence results from seasonal fluctuations of the condensation and evaporation rates – see Sec. 2.2.3.

Case 2: The external inflow *and* outflow rates will be given. The model calculates then the water storage fluctuations $V_i(t) \neq 0$ due to accumulation of excess water in the compartments. In other words, the water ingress in the upper compartments results in water pools at the lower Shelter levels.

The purpose of this section is to quantify the hydraulic couplings between adjacent compartments. This task is solved by using so-called splitting or distribution coefficients k_{ij} to "navigate" the water flow inside the Shelter. [A description based on conductivity's and Darcy-law is in principle possible but for this problem not adequate since the Shelter represents a heterogeneous system of porous media *and* fracture networks.]

The splitting coefficient k_{ij} (model input) is defined as the ratio of the transferred water amount from compartment $i \rightarrow j$ to the water amount in compartment i. Its value is therefore smaller or equal to one, $k_{ij} \leq 1$. Two compartments are isolated from each other if $k_{ij} = 0$; on the other hand, $k_{ij} = 1$ describes total discharge.

Tab. 3 Definition of the internal flow rates by splitting coefficients k_{ij}

	k_{ij}		k_{ij}		k_{ij}
CH→H2	0.13	S2→BR	0.40	EF→P2	1.00
CH→H1	0.13	PR→H1	1.00	H1→EF	0.26
CH→S2	0.19	BR→SC	0.56	H1→P2	0.74
CH→S1	0.19	BR→C1	0.22	H2→P2	1.00
CH→RS	0.27	BR→C2	0.22	P2→P1	1.00
CH→CW	0.09	C2→SC	0.58	CW→H2	0.25
RS→BR	1.00	C2→P2	0.42	CW→LB	0.75
S1→C1	0.60	C1→SC	0.58	IB→MH	1.00
S1→BR	0.40	C1→EF	0.42		
S2→C2	0.60	SC→P2	1.00		

The water flow within the Shelter was studied by tracer experiments in [T13]. Based on these results splitting coefficients k_{ij} (normalized to 1) for the compartment model are deduced. The obtained data are listed in Tab. 3. These data correspond to the flow paths (arrows) depicted in Fig. 6.

2.3 Chemical Processes

The goal of this section is to combine the above ideas to a generalized flowchart for the step-by-step simulation of the chemical transformations inside each compartment and for each time step of size Δt.

2.3.1 Kinetics versus Thermodynamic Equilibrium

In the model it will be distinguished between the following processes: kinetics, equilibrium calculations with PhreeqC, diffusion and mixing (see Tab. 4).

Tab. 4 Physico-chemical processes used in the model

process		main paramaters
kinetics	dissolution of primary phases	specific rate r, specific surface A^R
equilibrium	thermodynamic equilibrium calculations with PhreeqC; equilibrium between aqueous phase and both secondary minerals and gas phases	log k-values
diffusion	treated as mixing of two solutions which are in direct contact (mixing factors f depend on D)	diffusion coefficient D
mixing	mixing of different solutions, calculations with PhreeqC	mixing factors f

The interrelations of typical physico-chemical processes is demonstrated in Fig. 8:

- the dissolution of the *primary* phase (as a kinetic process) which is in contact with the stagnant water surrounding the phase as a thin film,
- the precipitation of *secondary* phases as a result of equilibrium calculations (with PhreeqC),
- the diffusion process between the stagnant water and mobile water,
- the mixing of the mobile water phase with incoming waters from other compartments and/or the outside.

In each time-step a quasi-equilibrium is assumed. The appropriate intensive parameters such as pH, and redox potential Eh are calculated with PhreeqC which includes:

- ion speciatiation and charge balance,
- activity coefficients from Davies or extended Debye-Hückel equation,,
- aqueous complexation,
- redox reactions,
- equilibrium with solid and gas phases,
- ion-exchange,
- sorption and surface-complexation.

The obtained intensive parameters (pH, Eh) influence the stability of phases and, in this way, the dissolution kinetics.

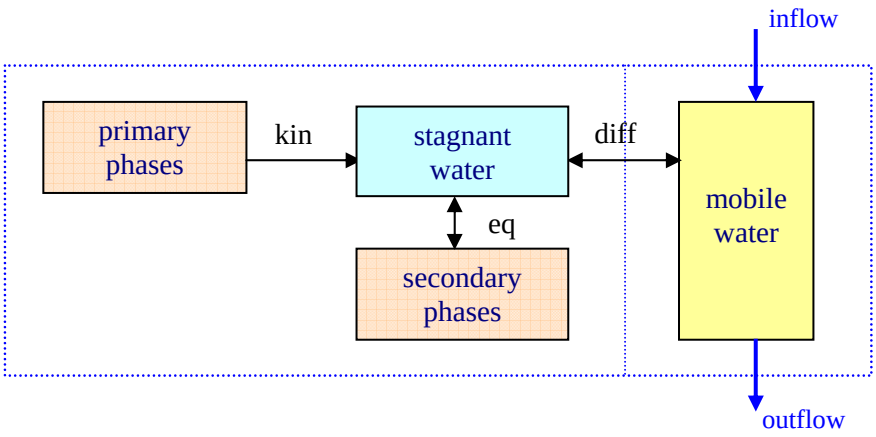

Fig. 8 Scheme of typical processes within one compartment: kinetics (kin), equilibrium processes (eq) and diffusion (diff)

The most important parameter for equilibrium calculations is the so-called equilibrium constant (log-k value) for each reaction which enters the mass-action equation. These data are stored in thermodynamic libraries (ASCII files). Data for Shelter-specific phases which are not included in common libraries (wateq4f.dat, etc.) will be deduced from GEM-calculations with help of Selektor-A code.

Formally, the dissolution and precipitation processes can be described either as an equilibrium approach (using PhreeqC) or as a kinetic approach. The advantage of the thermodynamic equilibrium approach is that for each phase only *one* parameter (log-k value) is necessary whereas the kinetic approach needs several parameters (rate constants r, hydrologic parameters like the reactive surface, etc.) which are difficult to measure. However, a major deficiency with equilibrium models is that minerals and other reactants often do not react to equilibrium in the time frame of a model period Δt. A kinetic approach is then required. For this reason, both approaches will be used in the dynamical compartment model as shown in Tab. 4.

Mathematically, the dynamics of phase transformations depicted in Fig. 8 will be described by a system of differential equations in Sec. 3.4.1.

2.3.2 Components of Shelter Waters

The chemical composition of a solution (Shelter water) is defined by the following parameters:

intensive parameters:	pH, Eh, T,
major constituents (> 5 mg/L):	Ca, Mg, Na, K, Si, C, S, Cl, P,
minor constituents (< 5 mg/L):	U, Al, Fe,
trace constituents:	Sr, Cs.

The water composition is determined by typical processes or several sources (see Tab. 5):

- equilibrium to air (O_2, CO_2),
- dissolution of primary solid phases (CM, DM, CF, LFCM, HP) which produces the solutes U, Ca, K, Na, Mg, Si, and other elements.

The thermodynamic equilibrium with secondary minerals serves as rate limiting processes: it acts as a “sink term” if supersaturation occurs.

Tab. 5 Origin and source of the Shelter-water components

component	origin or source
O	contact with air
C	contact with air; dumping material dolomite
Ca	phase CHS (and Arg-Str)
Mg	phase hydrotalcite
Na	dumping material Na_3PO_4
K	phase: ? (or “noise” KCl)
Si	phase CHS; (and LFCM dissolution)
Al	phase hydrotalcite
Fe	corrosion phase: hydrogoethite, hydromagnetite
Cl	phase in serpentine concrete ?
S	phase Arg-Str (gypsum ?)
P	dumping materials: Na_3PO_4

U	dissolution kinetics of FCM

The sources of Fe are mainly the corrosion products of the construction material “steel”: hydrogoethite, hydromagnite. The sources of Na and P is the dumping material Na_3PO_4 thrown from helicopters to smoother the reactor fire during the “Active Phase Accident Management Actions” [Sich94]. The list of the equilibrium phases acting as sources or as sinks is given in Sec. 4.2.1.

It should be noted, that there are some problems to identify exactly the sources of K, S and Cl inside the Shelter. If these elements are underestimated in the actual calculations a so-called initial background composition will be generated by adding salts such as NaCl, Na_2SO_4 and/or KCl. The amount of these chemicals will be adjusted to the observed data.

The trace constituents Sr and Cs are treated as so-called non-reactive tracer elements which will be dissolved from FCM and transported inside the Shelter. Tracer elements are not included into thermodynamic equilibrium calculations with PhreeqC.

2.3.3 Chemical Transformations inside a Compartment

Collecting all facts discussed above the main procedure for calculating the solid-aqueous interaction *within* one compartment can be defined. The general scheme is given in Fig. 9. It is the same for each compartment and contains all processes which subsequently will be calculated (principle of superposition). However, in the first model version only the dominant processes should be considered.

The general procedure is decomposed into six steps. After each step a typical solution (of the mobile aqueous phase) will be calculated which is numbered by 1 to 6.

<u>mobile aqueous phases:</u>

solution 1: solution after mixing of inflow waters from other compartments; equilibrium with air (gas phases: CO_2 and O_2),

solution 2: solution after diffusion exchange with stagnant water phase from cement pores (solution a),

solution 3: solution after diffusion exchange with stagnant water phase from unaltered nuclear fuel pores (solution b),

solution 4: solution after diffusion exchange with stagnant water phase from lava pores (solution c),

solution 5: solution subsequent to kinetic dissolution of hot particles,

solution 6: solution after evaporation and equilibrium with secondary uranium minerals SUM 2; (evaporation lead to increases in concentrations which are proportional to the amount of water that evaporates)

Solution 6 serves as the input water for adjacent compartments.

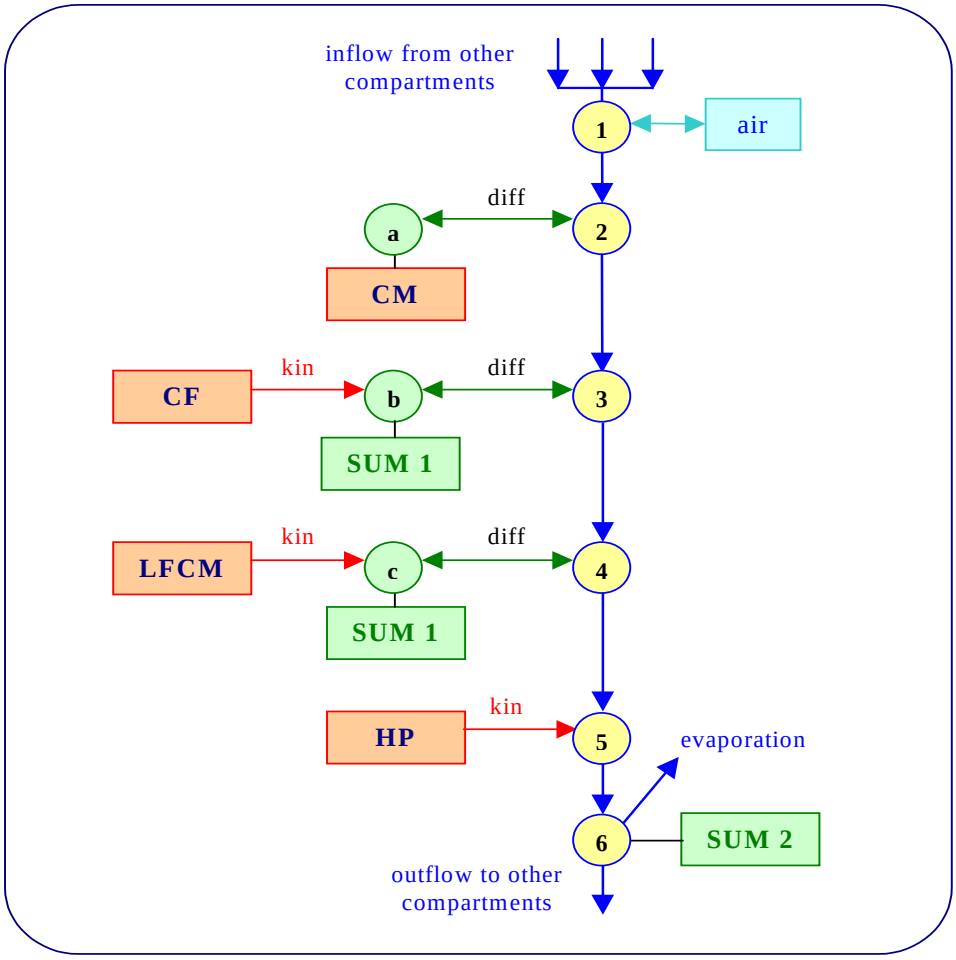

Fig. 9 General flowchart of chemical processes within one compartment which are performed at each time step of size Δt

In intermediate steps the pore solutions are calculated:

<u>stagnant aqueous phases (pore solutions):</u>

solution a: cement pore water which is in equilibrium with *cement* phases; the redox potential of this solution will be fixed to a realistic value (Eh ≈ -80 to –120 mV);

solution b: pore water or thin film of water surrounding the unaltered nuclear fuel fragments; the composition of this water is determined from:

- dissolution kinetics of UO_2,
- equilibrium with secondary uranium phases SUM 1,
- diffusion contact with mobile solution 2,

solution c: pore water or thin film of water surrounding the lava-like FCM with silicat-matrix; the composition of this water is determined from:

- dissolution kinetics of glass,
- equilibrium with secondary uranium phases SUM 1,
- diffusion contact with mobile solution 3.

The primary solid phases are the source for U and other components from the dissolution of construction materials and silicat glass matrix (Ca, K, Mg, Si, Al, Fe, S). The oxidation due to radiolysis of water will be included in an effective dissolution rate r_{eff} of the dissolution kinetics,

primary solid phases for FCM:

CF: UO_2 as unaltered nuclear fuel (core fragments),
LFCM: lava-like FCM with silicat-matrix,
HP: UO_{2+x} in hot particles,

primary solid phases for CM:

There are two main groups of construction materials: (a) concrete or cement phases and (b) phases of steel corrosion products.

Cement phases:

- amorphous calcium silicate hydrogel phase (CSH): CaH_2SiO_4
- hydrotalcite: $Mg_4Al_2O_7(H_2O)_{10}$
- solid-solution Arg-Str $(Ca,Sr)\ SO_4$

Phases for steel corrosion products:

- hydrogoethit: ...
- hydromagnetit: ...

secondary solid phases:

SUM 1: secondary uranium minerals:

- schoepite $UO_2 \cdot 2H_2O$,
- rutherfordine UO_2CO_3,
- uranophane $Ca[UO_2SiO_3OH]_2 \cdot 5H_2O$,
- phosphate $(UO_2)_3(PO_4)_2 \cdot 4H_2O$,

SUM 2: secondary uranium minerals:

- Na-autunite $Na_2(UO_2)_2(PO_4)_2$,
- natriumuranyltricarbonate $Na_4(UO_2)_2(CO_3)_3$.

Finally, the secondary phases gypsum, amorphous $Fe(OH)_3$, and amorphous $Al(OH)_3$ are included in all equilibrium calculations to avoid supersaturation of the corresponding solutes.

2.3.4 Relations between Kinetic Parameters for FCM

Assuming zero-order kinetics there are three specific rates [$mol \cdot m^{-2} \cdot s^{-1}$] for uranium:

r_{CF} for dissolution of unaltered fuel UO_2 from CF,
r_{LFCM} for dissolution of uranium from LFCM,
r_{HP} for dissolution of UO_{2+x} from HP,

and for silicium

r_{Si} for dissolution of Si from LFCM.

Obviously, from observations the following relations between dissolution rates can be qualitatively deduced:

$$r_{HP} >> r_{CF} \quad \text{and} \quad r_{HP} >> r_{LFCM},$$

which reflect the fact that the dominant dissolution process for U is the dissolution of (high-oxidized) nuclear fuel powder – HP. Therefore, in a first model version the uranium content in the Shelter water will be described by the dissolution of hot particles (and neglecting the LFCM and CF dissolution processes, $r_{CF} = 0$, $r_{LFCM} = 0$). Typical values for r_{HP} will be presented in Sec. 4.2.3.

2.3.5 Example: Water Percolation through the Shelter

Based on existing sample points a chain of compartments can be constructed to investigate the percolation of water downstream inside the Shelter (see Fig. 2):

PR ⇒ H1 ⇒ P2 ⇒ P1.

The location of the observation points inside the Shelter are given in Tab. 6. The corresponding average water compositions are listed in Tab. 7. Along the chain from the upper to the lower levels the uranium content in the water increases due to interactions with FCM. The rapid increasing of U from about 0.4 mg/L (in compartment H1) to 20 mg/L (in compartment P2) is caused by the fact that P2 obtains additional inflows from other compartments such as EF, SC and H2 (see Fig. 2). It is the object of the compartment model to combine *all* flow paths in the calculation while the above chain represents only a fragment of the flow pattern.

Tab. 6 Location of observation points inside the Shelter

point	compartment	room	axis	row	level [m]
12	PR	402/3	49-50	D – E	24.0
25	PR	402/3	49	D	18.5
14	H1	406/2	43-44	Zh – I	12.5
19	H1	219/2	42-43	M – N	6.0
6	P2	012/16	48-49	E – Zh	2.2
32	P1	012/7	47-48	E – Zh	-0.65

Tab. 7 Average water composition at the observation points (data from [T13])

compartment (point)	pH	CO_3 [mg/L]	HCO_3 [mg/L]	HPO_4 [mg/L]	U [mg/L]
PR (12)	8.8	75	519	15	0.13
PR (25)	9.5	510	1448	18	0.2
H1 (14)	9.3	667	2074	12	0.4
H1 (19)	9.3				0.34
P2 (6)	8.8	90	570	4	20
P1 (32)	9.0	210	750	4	23

From the chemical point of view the measured data in Tab. 7 are far from being complete for a detailed modeling (lack of major cations, no Eh, etc.). Thus it will be important for the model calibration to increase the number of measured element concentrations at the observation points (at least for the major components listed in Sec. 2.3.2).

3 Mathematical Model

In the present Chapter the conceptual model of Chapter 2 will be mapped onto mathematical equations. Many effort will be done to give a straightforward and clear derivation of the main equations. The obtained equations are the basis for:

- selecting the numerical algorithm and programming strategies,
- identification of the (free) model parameters and their combination with kinetic and hydrological quantities.

The compartment model is based on a coarse spatial discretization of the model space “Shelter” into N compartments (i = 1 to N) which are hydraulically connected. In each compartment i the mass and / or species concentration will be calculated as a function of time:

dynamics: $m_i = m_i(t)$ and / or $c_i = c_i(t)$.

Here the mass m_i and concentration c_i represent a vector of K chemical elements and species: $m_i = (m_i^{(1)}, m_i^{(2)}, \ldots, m_i^{(K)})$, $c_i = (c_i^{(1)}, c_i^{(2)}, \ldots, c_i^{(K)})$. Beginning with an initial configuration at t = 0, the evolution of the system will be performed in time steps of size Δt:

$m_i(t+\Delta t) = m_i(t) + \Delta m_i$ and / or $c_i(t+\Delta t) = c_i(t) + \Delta c_i$.

The changes in mass Δm and/or concentrations Δc are caused by reactive transport. The changes will be calculated in a stepwise procedure (operation splitting) including the following processes: transport, dissolution and precipitation kinetics, equilibrium processes with PhreeqC, diffusion between stagnant and mobile aqueous phases, etc.

The model bases on the principle of mass conservation which holds for both the compartment (local balance) and the total model space (global balance).

3.1 Basic Equations

In this section both the advection-reaction equation and the flow equation for the compartment model are derived from the principle of mass conservation. Due to the conceptual difference between the compartment model and the transport models in hydrogeology [DS98] the obtained equations differ in several respects from the common used equations in hydrogeology. The derived equations are the basis for the numerical model in Sec. 3.2.

3.1.1 Advection-Reaction Equation

Conservation of mass for a chemical that is transported yields:

change in mass storage with time = mass inflow rate – mass outflow rate + mass production rate

in units of mass per unit of time (MT^{-1}). This statement applies to a domain of any size, that is, for one compartment as well as for the whole system. Let us now consider the (mobile) aqueous phase in compartment i with mass $m_i^{aq} = c_i V_i$. The change in mass is then given by the

(9) advection-reaction equation:
$$\frac{dm_i^{aq}}{dt} = \left(\frac{dm_i}{dt}\right)_{adv} + V_i^R R_i ,$$

where the first term corresponds to the advection. The second term describes the fluid sink/source with $R_i = R_i(c_i)$ as the reaction rate in units ($ML^{-3}T^{-1}$) and V_i^R as the corresponding reaction volume (L^3). The sink/source term results from interactions with other subsystems (stagnant water domain and/or solid phases) and will be specified in Sec. 3.3.

The mass transport due to advection can be expressed by the

(10) advection equation:
$$\left(\frac{dm_i}{dt}\right)_{adv} = \sum_{j=0}^{N} \left[Q_{j\to i} c_j - Q_{i\to j} c_i \right] + (Q_i^{cnd} - Q_i^{evp})\, c^0 ,$$

where

$m_i^{aq} = c_i V_i$	element mass in mobile water of compartment i	M
V_i	volume of mobile water in compartment i	L^3
c_i	element concentration in mobile water of compartment i	ML^{-3}
c^0	element concentration in pure water (H_2O)	ML^{-3}
c_0	element concentration of external inflow water (rain water)	ML^{-3}
$Q_{i\to j}$	hydraulic flow rate from compartment i to compartment j	L^3T^{-1}
Q_i^{cnd}	condensation rate in compartment i	L^3T^{-1}
Q_i^{evp}	evaporation rate in compartment i	L^3T^{-1}.

Note, that all quantities are functions of time: c = c(t), Q = Q(t), V = V(t). The sum over j in Eq. (10) also includes the coupling to the environment or "outside region" of the Shelter (carrying the subscript 0):

$Q_{0\to i} = Q_i^{\text{ext in}}$ hydraulic inflow rate from outside to compartment i L^3T^{-1}

$Q_{i\to 0} = Q_i^{\text{ext out}}$ hydraulic outflow rate from compartment i to outside L^3T^{-1}.

In this way, the net inflow/outflow rate in compartment i is the sum of two contributions: the outside inflow/outflow (external coupling) and the inflow/outflow from other compartments (internal coupling):

(11) $$Q_i^{\text{in}} = Q_{0\to i} + \sum_{j=1}^{N} Q_{j\to i} = Q_i^{\text{ext in}} + Q_i^{\text{int in}} ,$$

(12) $$Q_i^{\text{out}} = Q_{i\to 0} + \sum_{j=1}^{N} Q_{i\to j} = Q_i^{\text{ext out}} + Q_i^{\text{int out}} .$$

Obviously, external inflow appears in the upper level compartments, whereas the external outflow is in the lower level compartments of the Shelter. The corresponding external flow rates are specified in Tab. 2. The distinction between external and internal flow is important since the external flow determines the internal flow field as a kind of time-dependent "boundary condition".

3.1.2 Flow Equation and Flow Field

Mathematically, the change in mass consists of two terms according to the product rule of a derivative:

(13) $$m_i = V_i\, c_i \quad \Rightarrow \quad \frac{dm_i}{dt} = c_i \frac{dV_i}{dt} + V_i \frac{dc_i}{dt} .$$

Using this product rule one obtains for the left-hand side of Eq. (9) the expression

(14) $$c_i \frac{dV_i}{dt} + V_i \frac{dc_i}{dt} = \sum_{j=0}^{N} \left[Q_{j\to i} c_j - Q_{i\to j} c_i \right] + \left[Q_i^{\text{cnd}} - Q_i^{\text{evp}} \right] c^0 + V_i^R R_i \quad .$$

For *constant* concentrations such as pure water, $c_i = c^0 = [H_2O]$, and in absence of reactions ($R_i = 0$), the above expression reduces to the

(15) flow equation: $$\frac{dV_i}{dt} = \sum_{j=0}^{N} \left[Q_{j\to i} - Q_{i\to j} \right] + \left(Q_i^{\text{cnd}} - Q_i^{\text{evp}} \right) ,$$

which is determined solely by the flow rates Q. The flow equation is a special case of the advection equation (10) applied for pure water transport.

If the water volume in all compartments is not changed, $dV_i/dt = 0$ for all i, we have $V_i(t) = \text{const} = V_i(0)$ and stationarity holds,

(16) steady state: $$\sum_{j=0}^{N} \left[Q_{j\to i} - Q_{i\to j} \right] + \left(Q_i^{cnd} - Q_i^{evp} \right) = 0 \quad .$$

For numerical purposes it is useful to rewrite the flow equation into the expanded form (for small Δt):

(17) $$V_i(t+\Delta t) = V_i(t) + \left(Q_i^{in} - Q_i^{out} + Q_i^{cnd} - Q_i^{evp} \right) \Delta t \,,$$

where the definitions in Eqs. (11) and (12) are incorporated.

Note that for finite Δt Eq. (17) is an approximation of the flow equation (15) which becomes exact if either $\Delta t \to 0$ or all Q's are time-independent. Formally, Eq. (17) is obtained by integration of the flow equation from t to $t+\Delta t$ supposing that all Q's are constant within the interval Δt. In practice the size of Δt depends on the time scale of Q-changes.

Calculation of the Flow Field. The internal flow field as a function of time is determined solely by the external flow rates including the time-dependent condensation and evaporation rates (time-dependent "boundary conditions"). The flow field will be calculated iteratively for every time step. In general, the following options are possible to describe the compartment-by-compartment flow:

- $Q_{i\to j} = L_{ij}\,(h_i - h_j)$ as a function of the hydraulic gradient Δh (Darcy-law like approach to flow in porous media or the flow in open drifts or raises); as input effective conductivities L_{ij} in units L^2T^{-1} are used,
- $Q_{i\to j}$ calculated by so-called splitting coefficients k_{ij} (input values with dimension 1),
- flow-field calculation as a combination of both methods (vertical flow by splitting coefficients; horizontal flow by conductivities).

To calculate the flow field in the Shelter, splitting coefficients rather than conductivities will be used. The splitting coefficients k_{ij} can be estimated from the ratio of the interface area of two adjacent compartments or from flow paths information's taken from tracer experiments, respectively. The flow rate between compartment i and j is then given by

(18) $$Q_{i\to j} = k_{ij} \left(Q_i^{int\,in} + Q_i^{cnd} - Q_i^{evp} \right) \qquad \text{with} \quad \sum_j k_{ij} = 1 .$$

Splitting coefficients for the Shelter system are listed in Tab. 3. [Accumulation of excess water occurs in compartment i if the condition $\sum_j k_{ij} < 1$ holds, respectively.]

3.1.3 Linkage between Flow and Transport

The changes in concentration, dc_i/dt, are obtained directly from Eq. (14) after replacing the term dV_i/dt by the flow equation (15). This yields the linkage between flow and transport in one expression:

(19) $$V_i \frac{dc_i}{dt} = \sum_{j=0}^{N} Q_{j\to i}(c_j - c_i) + \left(Q_i^{cnd} - Q_i^{evp} \right)\left(c^0 - c_i \right) + V_i^R R_i \,.$$

It is worth nothing that in this equation the outflow rates $Q_{i\to j}$ are disappeared. For further purposes Eq. (19) will be written in the expanded form (for small Δt):

$$(20) \qquad V_i c_i (t+\Delta t) = V_i c_i + \sum_{j=0}^{N} Q_{j\to i}(c_j - c_i)\,\Delta t + \left(Q_i^{cnd} - Q_i^{evp}\right)\left(c^0 - c_i\right)\Delta t + V_i^R R_i \Delta t .$$

The concentrations on the right-hand side are given at time t. Equation (20) together with Eq. (17) are the main formulas for the further numerical treatment in Sec. 3.2.

3.2 Numerical Model

Based on the above equations the numerical model can be defined. Thereby, the calculation of mass transport and mass transformations as a function of time will be performed iteratively for each compartment i and for each time step with steps of size Δt:

$$(21) \qquad m_i (t) \Rightarrow m_i (t+\Delta t) = V_i (t+\Delta t)\, c_i (t+\Delta t) .$$

This task is solved within a two-step algorithm which separates between flow and reactive transport:

- first step: $V_i (t) \Rightarrow V_i (t+\Delta t)$ and $Q_{i\to j}(t) \Rightarrow Q_{i\to j}(t+\Delta t)$ for $i,j \geq 1$,
- second step: $c_i (t) \Rightarrow c_i (t+\Delta t)$

using the following “start values”:

V_i (t=0)	and	c_i (t=0)	(initial condition),
$Q_i^{ext\ in}$ (t)	and	$Q_i^{ext\ out}$ (t)	(“boundary condition”).

The time-dependent “boundary conditions” also contain the condensation and evaporation rates.

In the *first step*, the water volume and the internal flow field (including all $Q_{i\to j}$ for $i,j \geq 1$) are calculated for time $t+\Delta t$ using Eq. (17) – the flow equation in the expanded form. Based on the obtained quantities V_i and $Q_{i\to j}$, in a *second step* the concentrations are calculated by Eq. (20).

The second step is performed using the “mixing operation” of a thermodynamic model (equilibration calculation with PhreeqC). However, to calculate $c_i(t+\Delta t)$ by Eq. (20) two cases should be distinguished:

- case 1: $V_i > 0$ (flow through not-empty compartments),
- case 2: $V_i = 0$ (flow through empty compartments).

For example, case 1 describes the situation for the low-lying compartments located near the earth surface in which water is accumulated in pools. On the other hand, case 2 describes the common situation for the upper-level compartments where water flows through “empty com-

partments" without accumulation of excess water. To avoid zero volumes in Eq. (20), the following assumption should be made in case 2:

(22) $$V_i = (Q_i^{in} + Q_i^{cnd} - Q_i^{evp})\,\Delta t \qquad \text{if} \qquad V_i = 0,$$

which is indeed zero if $\Delta t \to 0$. In this way, for both cases the following "mixing formula" is obtained from Eq. (20):

(23) $$c_i\,(t+\Delta t) = (1 - f_i)\,c_i + \sum_{j=0}^{N} f_{ij}\,c_j + \frac{V_i^R}{V_i} R_i\,\Delta t$$

with the mixing factors:

(24) $$f_{ij} = \frac{Q_{j\to i}}{V_i}\,\Delta t \qquad \text{and}$$

(25) $$f_i = \sum_{j=0}^{N} f_{ij} + \frac{Q_i^{cnd} - Q_i^{evp}}{V_i}\,\Delta t = \frac{Q_i^{in} + \left(Q_i^{cnd} - Q_i^{evp}\right)}{V_i}\,\Delta t$$

(which holds for concentrations different from H_2O, i. e., for $c_i \neq c^0$). In case 2 the above mixing equation further reduces to:

(26) $$c_i\,(t+\Delta t) = \sum_{j=0}^{N} f_{ij}\,c_j + \frac{V_i^R R_i}{Q_i^{in} + Q_i^{cnd} - Q_i^{evp}}\,.$$

Whereas Eq. (23) is appropriate for compartments containing water pools with volume V_i = const (stationary pool) or $V_i = V_i(t)$ (temporary pools), Eq. (26) holds for compartments *without* water pools.

3.3 Sink/Source Term

In general, the source term in Eq. (9) can be used to describe any kinetic process or non-advective mass exchange with other subsystems. In Sec. 3.3.1 we will consider both dissolution and diffusion processes and discuss the structure of the corresponding rate equations. In Sec. 3.3.3 the dissolution/precipitation processes are described by an equilibrium approach.

3.3.1 Diffusion and Dissolution Processes

The overall reaction rate R_i and reaction volume V_i^R in the advection-reaction equation (9) should be replaced by R_i^S, V_i^S in case of dissolution kinetics or by R_i^D, V_i^D in case of diffusion processes, respectively, for which the following expressions hold:

(27) dissolution: $$R_i^S = \frac{r}{a_S}\left(\frac{m_i^s(t)}{m_i^s(0)}\right)^{\gamma} \qquad \text{with} \qquad a_S = \left(\frac{V_i^S}{A_i^S}\right),$$

(28) diffusion: $R_i^D = \frac{D}{a_D^2}\left(\tilde{c}_i - c_i\right)$ with $a_D = \left(\frac{V_i^D}{A_i^D}\right)$.

The quantities are:

R_i^S	overall reaction rate for dissolution	$ML^{-3}T^{-1}$
R_i^D	diffusion rate	$ML^{-3}T^{-1}$
r	specific rate for dissolution	$ML^{-2}T^{-1}$
D	diffusion coefficient	L^2T^{-1}
V_i^S	"reactive" water volume in contact with the solid	L^3
V_i^D	volume of "diffusion layer" (between stagnant and mobile water)	L^3
A_i^S	(initial) surface area of the solid which is in water contact	L^2
A_i^D	surface of "diffusion layer" (between stagnant and mobile water)	L^2
c_i	concentration in the *mobile* aqueous phase	ML^{-3}
$\tilde{c}_i$	concentration in the *stagnant* aqueous phase	ML^{-3}
$m_i^s(t)$	moles of solid at given time t in compartment i	M.

The last factor in the expression for R_i^S in Eq. (27) is named demolition factor. It accounts for changes in the size during dissolution and also for selective dissolution and aging of the solid. For uniformly dissolving spheres and cubes $\gamma = 2/3$. For large mass supply the demolition factor in round brackets can be set equal to 1.

In both cases the overall reaction rate R_i is decomposed into a "geometrical factor", a_S and a_D, and a material-specific constant: the reaction rate r or the diffusion coefficient D. It should be noted, that whereas A_i^D, V_i^D, A_i^S, and V_i^S are depend on (the mass deposit of) compartment i the parameters a_D and a_S are independent of i.

The stagnant water volume which is in direct contact with the solid matrix can be approximated by the volumetric water content θ (moisture content in units L^3/L^3) and the volume of the solid, m_i^s / ρ_s:

(29) $$V_i^s = \theta \frac{m_i^s}{\rho_s},$$

where ρ_s represents the bulk density of the solid in units ML^{-3}. If the pores of the matrix are totally filled with water the quantity θ becomes equal to the porosity n, that is $\theta \le n$. Thus, for saturated media θ should be replaced by n in the above equation.

Another important parameter is the specific surface area $A_s = A_i^S / m_i^s$ in m^2/g (or $m^2/100$ g solid medium), which can be measured by BET method. Note, that the specific quantity A_s is independent of the compartment number i. In this way, the above parameter a_S can be expressed by

(30) $$a_S = \frac{\theta}{\rho_s A_s}.$$

Once more it reflects the fact that a_S is a specific quantity which is independent of the compartment number i.

3.3.2 First-Order Kinetics

The specific rate r for a given substance can be a constant (zero-order kinetics) or a linear function of the concentration (first-order kinetics). As a special kind of first-order kinetics the following rate is often applied [PA99]:

(31) $$r = r_0 \left[1 - \left(\frac{IAP}{k} \right)^{\sigma} \right],$$

where r_0 is an empirical constant and IAP/k is the saturation ratio. This rate equation can be derived from transition-state theory (TST), where the coefficient σ is related to the stoichiometry of the reaction when an activated complex is formed (often $\sigma = 1$). An advantage of this expression is that it applies for both supersaturation and undersaturation, and the rate is zero at equilibrium. The rate is constant over a large domain whenever the geochemical reaction is far from equilibrium (IAP/k > 0.1), and the rate approaches zero when IAP/k approaches 1.0 (equilibrium).

The diffusion process in Eq. (28) is treated as a kind of first-order kinetics which depends on the concentration difference between the two adjacent aqueous phases. Directly measured values for diffusion of ions in aqueous solutions are in the order $D \approx 10^{-5}$ cm^2/s [AP93]. A model assumption is that the diffusion coefficient D is approximately equal for all species.

3.3.3 Water-Solid Equilibrium

As was already discussed, the fast dissolution/precipitation processes can be described by using thermodynamic equilibrium models if the appropriate dissolution constant (log-k value) is known. Within the dynamical compartment model this method will be used to describe the interaction of stagnant waters with minerals, respectively. At each time step a so-called quasi-equilibrium is assumed.

Equilibrium processes – which naturally does not contain the time-parameter t – can formally be mapped onto a dynamical description with sink/source terms like in Eq. (9). This is done by using Dirac's delta-function, $\delta(t-t_{eq})$, for the overall "reaction rate":

(32) equilibrium: $$R_i^{eq} = \left(c^{eq} - c_i \right) \delta (t - t_{eq}),$$

where t_{eq} denotes the equilibration time, and c^{eq} refers to the concentration of the species which is in equilibrium with the solid phase. Both quantities are related by $c_i(t_{eq}) = c^{eq}$. The equilibrium concentration c^{eq} is independent of i; it will be obtained from PhreeqC-calculations.

3.4 Dynamics of Phase Transformations

So far only *one* phase, the mobile water phase, was considered in the advection-reaction equation. In the following the dynamics of transformations between several phases depicted in Fig. 8 will be described by a system of differential equations. From the final expressions the model parameters or parameter-combinations will be deduced in Sec. 3.4.2.

The derived equations describe the *general* case (diffusion + dissolution kinetics + equilibrium processes). As was shown in Fig. 9, both the dissolution of hot particles (no stagnant water) and the dissolution of construction materials (no kinetics) are *special* cases. The dissolution of HP will be described in Sec. 3.4.3.

3.4.1 Interacting Subsystems

Let us consider a subsystem of one mass type (CF, LFCM or CM). The element mass m_i within one compartment i is distributed over four phases,

(33) $$m_i(t) = m_i^{s1} + m_i^{s2} + m_i^{aq} + \tilde{m}_i^{aq},$$

where

m_i^{s1}	element mass in the solid phase of primary mineral	M
m_i^{s2}	element mass in the solid phase of secondary mineral	M
$m_i^{aq} = c_i V_i$	element mass in the *mobile* aqueous phase (bulk water)	M
$\tilde{m}_i^{aq} = \tilde{c}_i \tilde{V}_i$	element mass in the *stagnant* aqueous phase (pore water)	M
V_i	volume of mobile water (bulk water)	L^3
$\tilde{V}_i$	volume of stagnant water (pore water)	L^3

The dynamics of mass exchange between these phases is given by a system of four differential equations:

(34) $$\frac{dm_i^{aq}}{dt} = \left(\frac{dm_i}{dt}\right)_{adv} + V_i^D R_i^D,$$

(35) $$\frac{d\tilde{m}_i^{aq}}{dt} = -V_i^D R_i^D + V_i^S R_i^S - V_i^S R_i^{eq},$$

(36) $$\frac{dm_i^{s1}}{dt} = -V_i^S R_i^{S1},$$

(37) $$\frac{dm_i^{s2}}{dt} = V_i^S R_i^{eq}.$$

Here the mobile water phase is coupled to the stagnant water phase by diffusion; the stagnant water phase is coupled to both the solid phase by dissolution kinetics and the secondary minerals by equilibrium thermodynamics (see Fig. 8). The corresponding “reaction rates” are

taken from Eq. (27), Eq. (28) and Eq. (32). The advection term which describes the mass transport to other compartments and/or to the environment is expressed in Eq. (10). [To keep these equations transparent all stoichiometry coefficients are neglected in the notation, but they are included in calculations.]

To reduce the number of free parameters the following assumption will be made: First, the space of the "diffusion layer" and "reactive dissolution volume" are identified as the volume of stagnant or pore water: $V_i^D = V_i^S = \tilde{V}_i$. Second, the layer thickness or inverse specific surface should be equal: $a_D = a_S = a$. Third, the precipitated secondary mineral does not influence the surface of the primary mineral. These assumptions lead to the following expressions:

(38) $$\frac{dm_i^{aq}}{dt} = \left(\frac{dm_i}{dt}\right)_{adv} + \tilde{V}_i \frac{D}{a^2}\left(\tilde{c}_i - c_i\right),$$

(39) $$\frac{d\tilde{m}_i^{aq}}{dt} = -\tilde{V}_i \frac{D}{a^2}\left(\tilde{c}_i - c_i\right) + \tilde{V}_i \frac{r}{a}\left(\frac{m_i^{s1}(t)}{m_i^{s1}(0)}\right)^{\gamma} + \tilde{V}_i \left(c^{eq} - c_i\right) \delta\left(t - t^{eq}\right).$$

According to Eq. (29) the stagnant water volume can be expressed by the volumetric water content θ (or porosity n for saturated media) and the bulk density ρ_s. Using both Eq. (29) and Eq. (30) one gets the following parameter reduction:

(40) $$\frac{\tilde{V}_i}{a} = m_i^s A_s,$$

where the parameters θ and ρ_s are cancelled.

3.4.2 Final Expressions and Model Parameters

From Eq. (38) and Eq. (39) the following expressions for the concentrations in the mobile and stagnant aqueous phases are obtained

(41) $$c_i(t+\Delta t) = \left(1 - f_i - \frac{\tilde{V}_i}{V_i} g\right) c_i + \sum_{j=0}^{N} f_{ij} c_j + \frac{\tilde{V}_i}{V_i} g\, \tilde{c}_i$$

(42) $$\tilde{c}_i(t+\Delta t) = C_i - (C_i - c^{eq})\,\Theta(C_i - c^{eq})$$

with the abbreviation

(43) $$C_i = (1 - f_i - g)\,\tilde{c}_i + g c_i + \frac{r}{a}\Delta t$$

and the Heaviside step-function Θ(x) which results from integrating the Dirac's delta-function to simulate the equilibrium processes:

(44) $$\Theta(x-a) = \begin{cases} 1 & \text{for } x \geq a \\ 0 & \text{for } x < a \end{cases}.$$

The equilibrium concentration c^{eq} depends on the chemical milieu of the pore water (including pH and Eh values) as well as on the dissolution constant (log-k value); c^{eq} will be calculated by PhreeqC.

Let us focus to Eq. (41). It is a special form of Eq. (23) with the following abbreviation for the diffusion process

(45) $$g = \frac{D}{a^2}\Delta t\,.$$

Equation (41) consists of three terms, where the second term accounts for the coupling to other compartments and/or the boundaries (external waters), and the third term describes the coupling to the stagnant water phase.

The final expressions in form of Eqs. (41) to (43) allow the extraction of the main model parameters or combinations of them. Thereby, the most influencing factors affecting the transformation process of a mineral or solid phase define one parameter set. For example, a parameter set is given by the following three quantities:

parameter set: D/a^2 , r/a , and $\tilde{V}_i = \theta\, m_i^{s1} / \rho_s\,.$

3.4.3 Special Case: Dissolution of Hot Particles

The derived expressions become much more simpler in the special case of direct dissolution of hot particles in the mobile water (without diffusion processes from the stagnant water; see HP-dissolution in Fig. 9). Using the first-order kinetics for HP-dissolution reported in [Kp00] the system of differential equations for the aqueous and solid phases reduces to

(46) $$\frac{dm_i^{aq}}{dt} = \left(\frac{dm_i}{dt}\right)_{adv} + \kappa\theta\, m_i^{HP},$$

(47) $$\frac{dm_i^{HP}}{dt} = -\kappa\theta\, m_i^{HP}\,.$$

Here, κ represents the first-order kinetic parameter in units T^{-1}, which depends on both the oxidation state of the fuel particles and the pH of the solution [Kp00]. The factor θ accounts for the fact that only a fraction of the total material deposit located in a compartment gets contact with water. [In hydrogeology which considers the transport in porous media θ represents the moisture content (unsaturated case) or the porosity (saturated case).]

The iterative algorithm to calculate the time-dependent concentration and mass is then given by the simple expressions:

(48) $$c_i(t+\Delta t) = \left(1 - f_i\right) c_i + \sum_{j=0}^{N} f_{ij}\, c_j + \frac{\kappa\theta\,\Delta t}{V_i}\, m_i^{HP}$$

(49) $$m_i^{HP}(t+\Delta t) = (1 - \kappa\theta\,\Delta t)\, m_i^{HP}\,.$$

The parameterization of κ will be given in Sec. 4.2.3; a first application of these formulas to estimate the parameters is given in Sec. 4.3.2.

3.4.4 Local and Global Mass Balance

The dynamical compartment model was derived from the principle of mass balance. This Section illustrates the local and global mass balance. The *local* mass balance holds for each compartment i and can be obtained by the time derivative of Eq. (33) which leads to

$$\frac{dm_i}{dt} = \frac{dm_i^{s1}}{dt} + \frac{dm_i^{s2}}{dt} + \frac{dm_i^{aq}}{dt} + \frac{d\tilde{m}_i^{aq}}{dt} = \left(\frac{dm_i}{dt}\right)_{adv} . \tag{50}$$

Here all source terms are cancelled. In other words, the net mass change in the compartment i is equal to the advective mass transport which exchanges mass with other compartments and/or with the environment.

Taking the sum over all compartments in Eq. (50) we get for the total model space “Shelter” the *global* mass balance

$$\frac{dm}{dt} = \sum_{i=1}^{N} \frac{dm_i}{dt} = \sum_{i=1}^{N} \left[Q_i^{ext\ in} c_0 - Q_i^{ext\ out} c_i \right] + \sum_{i=1}^{N} \left[Q_i^{cnd} - Q_i^{evp} \right] c^0 \quad , \tag{51}$$

which obviously does not include the internal couplings $Q_{i\to j}$ for i, j ≥ 1. Note that in deriving Eq. (51) from Eq. (9) the following identity for the internal flows was used:

$$\sum_{i=1}^{N} \sum_{j=1}^{N} \left[Q_{j\to i} c_j - Q_{i\to j} c_i \right] = 0 . \tag{52}$$

For a “closed system” (no external couplings: $Q_{0\to i} = Q_{i\to j} = 0$) the above equation reduces to the stationary case dm/dt = 0 (perfect isolated Shelter).

4 Data Preparation and Model Calibration

4.1 Input Data Structure

The model calculations base on the following geometrical and hydraulic input data:

- geometrical data (size and location of compartments) see Tab. 1,
- hydraulic data I (external flow rates) see Tab. 2,
- hydraulic data II (splitting coefficients for internal flow field) see Tab. 3.

The chemical input data are contained in two groups:

- thermodynamic data for equilibrium calculations (log-k values) contained in libraries,
- kinetic data.

The ASCII-file named `wateq4f.dat` contains thermodynamic data for the aqueous species as well as the gas and mineral phases [BN91]. Data for Shelter-specific phases will be obtained from Selektor-A-calculations (see Sec. 4.2.1).

4.2 Model Parameters

4.2.1 Thermodynamic Data

The following mineral phases will be included in the chemical modeling using PhreeqC (option `EQUILIBRIUM_PHASES`):

- Phases to simulate the construction materials (CM) concrete and steel in Tab. 8,
- Phases to simulate the secondary uranium minerals (SUM) in Tab. 9,
- Phases to avoid supersaturation in Shelter waters in Tab. 10,

The phases for CM are *sources* for Shelter-water components (primary phases), therefore their initial amount [mol] will be chosen sufficiently large. The other two types of equilibrium phases operate as *sinks* if supersaturation occurs, therefore their initial amount will be set equal to zero (secondary phases).

Tab. 8 Equilibrium phases to simulate the construction materials (CM): concrete and steel corrosion products

phase	reaction	log k	Ref
CSH	CaH_2SiO_4 ... = ...		A
Arg-Str	$(Ca,Sr)SO_4$ ...		A
portlandite	$Ca(OH)2 + 2H^+ = Ca^{+2} + 2H_2O$	22.8	W
hydrotalcite	$Mg_4Al_2O_7(H_2O)_{10}$		A
phase with K	K_2O ?		A
phase with Cl	in serpentine concrete ?		A
hydrogoethite	Fe... ?		A
hydromagnetite	Fe... ?		A

There are the following references for the data shown in the tables: A – Selektor-A code calculations, W – from library wateq4f.dat [BN91], S – from [SG94]. The abbreviation CSH names the amorphous calcium silicate hydrogel phase.

Tab. 9 Equilibrium phases to simulate the secondary uranium minerals (SUM)

phase	reaction	log k	Ref
schoepite	$UO_2(OH)_2 \cdot H_2O + 2H^+ = UO_2^{2+} + 3H_2O$	5.404	W
rutherfordine	$UO_2CO_3 = UO_2^{2+} + CO_3^{2-}$	-14.450	W
becquerellite	$CaU_6O_{19} \cdot H_2O + 14H^+ = Ca^{2+} + 6UO_2^{2+} + 18H_2O$	43.7	S
uranophane	$Ca(UO_2)_2(SiO_3OH)_2 + 6H^+ = Ca^{2+} + 2UO_2^{2+} + 2H_4SiO_4$	17.489	W
Na-autunite	$Na_2(UO_2)_2(PO_4)_2 = 2Na^+ + 2UO_2^{2+} + 2PO_4^{3-}$	-47.409	W
Na4UO2(CO3)3	$Na_4(UO_2)_2(CO_3)_3 = UO_2^{2+} + 3CO_3^{-2} + 4Na^+$	-16.290	W
(UO2)3(PO4)2:4w	$(UO_2)_3(PO_4)_2 \cdot 4H_2O = 3UO_2^{2+} + 2PO_4^{3-} + 4H_2O$	-37.4	W

Note, that schoepite $UO_2(OH)_2 \cdot H_2O$ is chemically equivalent to $UO_3 \cdot 2H_2O$. In practice there are different kinds of schoepite (schoepite I, II, and III, meta, para etc.).

Tab. 10 Secondary phases to avoid supersaturation in Shelter waters

phase	reaction	log k	Ref
gypsum	$CaSO_4 \cdot 2H_2O = Ca^{2+} + SO_4^{2-} + 2H_2O$	-4.58	W
$Fe(OH)_3$(a)	$Fe(OH)_3 + 3H^+ = Fe^{3+} + 3H_2O$	4.891	W
$Al(OH)_3$(a)	$Al(OH)_3 + 3H^+ = Al^{3+} + 3H_2O$	10.8	W

4.2.2 Kinetic Data

In contrast to the thermodynamic data the kinetic data are most often less known and difficult to determine. Kinetic processes depend upon many variables or parameters, one example for a parameter set was given in Sec. 3.4.2. Thus we need for *each* material which dissolves the appropriate quantities.

In a first model version we focus to the dominant U-dissolution process which is caused by the contact of water with the nuclear fuel powder (hot particles). The corresponding dissolution rate is discussed subsequently in Sec. 4.2.3. On the other hand, the dissolution of the CM-phases will be treated indirectly by putting the pore water in (quasi-) equilibrium with the appropriate cement phases listed in Tab. 8.

One crucial point in modeling the transformation processes is the estimate for the fraction of the material masses which is in contact with the aqueous phase. In hydrogeology which deals mainly with porous media this fraction is given by the volumetric water content θ. However, the situation is more difficult for the Shelter model where the movement of water inside the compartments is quite different from the flow through a homogenous medium. Therefore the quantity θ which characterizes the fraction of mass which is in contact with water should be estimated. That is:

in hydrogeology: θ = volumetric water content ($\leq$ porosity n),

in compartment model: $\theta = \dfrac{\text{mass in contact with water}}{\text{total mass}}$.

Note that θ depends on both the compartment i and the mass type (cement, lava, or hot particles etc.). A crude estimation for θ^{HP} will be given in Sec. 4.3.2.

Finally, the diffusion between the mobile and immobile water phases is also described by a first-order kinetic mass transfer. As a rule of thumb it will be characterized by the

overall diffusion coefficient: $D = 10^{-5}$ cm^2/s.

4.2.3 Dissolution Rate for Hot Particles

In [Kp00] the dissolution kinetics of fuel particles was determined in solutions of different acidities, using material obtained by crushing actual irradiated Chernobyl fuel, UO_2, and by its oxidation in air at a temperature of 670 K leading to UO_{2+x}. The radionuclide leaching rates from fuel particles are dependent on both the physico-chemical characteristics of particles and environmental conditions. Thus, the dissolution rate (T^{-1}) for first-order kinetics depends on the oxidation state and solution acidity (pH value):

(53) $$\kappa = a\left(10^{-\alpha\,pH} + \frac{\alpha}{\beta}\,10^{-7(\alpha+\beta)}\,10^{\beta\,pH}\right)$$

with the parameters

$a = 9 \pm 4$ year^{-1}	$\alpha = 0.5 \pm 0.1$	$\beta = 0.6 \pm 0.2$	for low-oxidized HP,
$a = 23 \pm 5$ year^{-1}	$\alpha = 0.35 \pm 0.05$	$\beta = 0.3 \pm 0.1$	for high-oxidized HP.

The parameter κ enters the system of differential equations (46) and (47). To compare the HP-dissolution rate with data from other references we re-calculate the specific reaction rate for HP which enters Eq. (27):

(54) $$r_{HP} = \kappa\,\rho_s\,a_S = \kappa\,\frac{\theta}{A_s},$$

where $\rho_s = (10.5 \pm 0.9)$ g/cm^3 is the density of uranium dioxide, UO_2. To estimate r_{HP} the following assumptions are made: $A_s = 0.06$ m^2/g for UO_2 powder measured by BET method [DA95], and $\theta \approx 0.1$ (about 10 % porosity). Thus we get for pH = 9 the following rates:

$\kappa = 0.038$ year^{-1}	$r_{HP} = 0.2$ mg m^{-2}day^{-1}	for low-oxidized HP,
$\kappa = 0.395$ year^{-1}	$r_{HP} = 1.8$ mg m^{-2}day^{-1}	for high-oxidized HP.

These rates should be compared with the dissolution rates 1.5 – 5.5 mg/m^{2}d (Gray et al. [Gr94]) and 2.4 ± 0.8 mg/m^{2}d (Bruno et al. [Br95a]) for UO_2. These values can also be compared with the dissolution rate of fuel samples taken from the Central Hall in water: 5 mg/m^{2}d [T13].

According to [Kp00] the most significant factor influencing the HP dissolution rate is the oxidation state of particles. Oxidation causes superficial cracking of the particles which greatly increases their surface and, therefore, their dissolution rate (by an order of magnitude as shown in the above example for low-oxidized and high oxidized HP).

4.3 Model Calibration

After explanation of the calibration strategy in Sec. 4.3.1 an example for the nuclear fuel dissolution will be given in Sec. 4.2.3.

4.3.1 Calibration Strategy

After construction of the model software by combining available tools and modules (including PhreeqC) the model will be calibrated. The model calibration will be performed in several steps. It consists of (a) the adjustment of the hydraulic and geometry data which determine the water flow and material deposit and (b) the adjustment of the chemical parameters for equilibrium and kinetic processes.

Concerning the chemical parameters, in a first step the major components (Ca, Na, K, Mg, C, S, O, Cl) as well as the chemical milieu (pH and Eh) of the Shelter water will be reconstructed by the following processes:

- water contact with atmospheric gas (CO_2, O),
- interaction of water with concrete phases to obtain an chloride-bicarbonate, potassium-sodium, alkaline, mildly reducing water type.

In a second step this type of water gets contact to the fuel containing materials which leads to the appearance of uranium in the water. This process is two-fold:

- dissolution of U from oxidized nuclear fuel powder (mainly hot particles – HP),
- rate limitation of U due to the precipitation of secondary uranium minerals (SUM).

The model will be tested on measured data (water compositions) at different observation points. To test the calculated flow pattern the measured activities of tracer elements (Sr^{90} and Cs^{137}) can be used.

4.3.2 Example: Dissolution of Hot Particles

In this section a first estimate for the U-concentration in Shelter waters due to dissolution of hot particles will be done. As shown in Fig. 10, an inflow of pure water into the under-roof compartments PR and CH of the Shelter is assumed which gets contact to the nuclear fuel powder. The calculation is based on Eq. (48) using the abbreviations $c_i(t+\Delta t) = [U]$ for the U-concentration, $c_i(t) = 0$, and $V_i = Q\Delta t$ which yields:

$$[U] = \frac{\kappa\,\Delta t}{V_i}\,\theta\, m_i^{HP} = \frac{\kappa}{Q}\,\theta\, m_i^{HP}. \tag{55}$$

Taking the parameters of Sec. 4.2.3, that is $\kappa = 0.038$ to $0.395\ year^{-1}$ and $\theta = 0.1$, and the HP-masses from Tab. 1 as well as the inflow rates from Tab. 2 an upper limit for the U-concentration in the Shelter water is obtained.

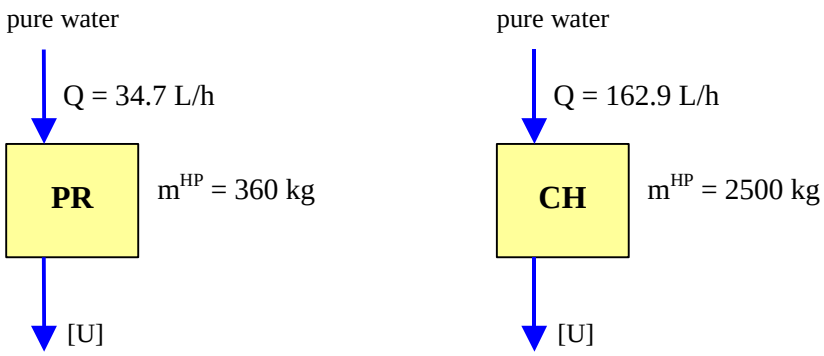

Fig. 10 Dissolution of HP in two upper-level compartments: PR and CH

The results are presented for low-oxidized and high-oxidized fuel particles in Tab. 11. These values overestimate the measured data for two reasons: First, during the downward flow the water gets contact only with a small fraction of the total amount of m^{HP} in a compartment: The situation is quiet different from water flow through porous media in hydrogeology where θ represents the porosity. Adittionally, in the Shelter there is also an uncontrolled flow in channels or fractures near the walls etc. Therefore the parameter θ should account for such effects by reducing its value. This crude estimation show that $\theta^{HP} < 0.1$. Second, in this calculation no precipitation of secondary uranium minerals is taken into account.

Tab. 11 Upper limits for U in water of compartments PR and CH due to dissolution of low-oxidized and high-oxidized HP (no U-precipitation is taken into account)

compartment	mass of HP [kg]	water inflow rate [L/h]	U-concentration [mg/L]
PR	360	34.7	4 ... 47
CH	2500	162.9	7 ... 69

[Note, that from both Eq. (54) and Eq. (55) the common formula for the dissolution rate in flow experiments [Br95a, Ca94] can be derived: $r = [U]Q/S$, where $S = mA_s$ is the total surface.]

5 Conclusion and Outlook

In this report a model concept – including the mathematical framework and numerical algorithm – is presented for the dynamical description of chemical FCM-transformations due to the influence of water and atmosphere which results in a redistribution of contaminants inside the Shelter. It takes into account as much as possible existing data for FCM and Shelter waters as well as for existing structures (premises) and established paths for water flows inside the Shelter.

The importance of such model for

- understanding the contamination of Shelter waters (evolution history),
- the prediction of medium and long term behavior of FCM inside the Shelter, and
- the development of an optimized active leaching strategy (in case if this technology will be applied for LFCM removal)

is evident.

The measured element concentrations at the observation points (see Tab. 7) are far from being complete for a detailed chemical modeling (lack of major cations, no Eh, etc.). Thus it will be important for the model calibration to increase the number of measured element concentrations at the observation points (at least for the major components listed in Sec. 2.3.2).

References

[AP93] Appelo, C.A.J., D. Postma: Geochemistry, Groundwater and Pollution, A.A. Balkema, Rotterdam 1993.

[BN91] Ball, J.W. and Nordstrom, D.K., WATEQ4F – User's manual with revised thermodynamic data base and test cases for calculating speciation of major, trace and redox elements in natural waters, U.S.G.S. Open-File Report 90-129, 185 p, 1991.

[Bo99] Bogatov, S.A. et al.: The Water Problem in the Object "Shelter", report (in russian) UDK 621.039.58 (1999).

[Br95] Bruno, J., J. de Pablo, L. Daro, E. Figuerola: Experimental study and modeling of the U(VI)Fe(OH)$_3$ surface precipitation/coprecipitation equilibria, Geochem. Cosmochem. Acta 59 (20) 4113-4129 (1995)

[Br95a] Bruno, J., I. Casas, E. Cera, J. de Pablo, J. Gimenez, M.E. Torrero: Uranium(IV) dioxide and SIMFUEL as chemical analogues of nuclear spent fuel matrix dissolution. A comparison of dissolution results in a standard NaCl/NaHCO$_2$ solution, Mat. Res. Soc. Proc. Vol. 353 (1995) 601.

[Ca94] Casas, I., J. Gimenez, V. Marti, M.E. Torrero, J. de Pablo: Kinetic Studies of Unirradiated UO_2 Dissolution under Oxidizing Conditions in Batch and Flow Experiments, Radiochimica Acta 66/67, 23-27 (1994)

[CB98] C++Builder 3 Visual Component Library Sprachreferenz Band 1 und 2, Borland GmbH 1998.

[CB99] Borland C++Builder 4 Entwicklerhandbuch, Inprise GmbH, Langen 1999.

[Ch98] The Shelter's Current Safety Analysis and Situation Development Forecasts (updated version), Tacis services DG IA, European Commission, November 1998.

[DA95] Diaz-Arocas, P., J. Quinones, C. Maffiotte, J. Serrano, J. Garcia, J.R. Almazan, J. Esteban: Effect of secondary phases formation in the leaching of UO_2 under simulated radiolytic products,Mat. Res. Soc. Symp. Proc. Vol. 353 (1995) p. 641

[DS98] Domenico, A.P., F.W. Schwartz: Physical and Chemical Hydrogeology, John Wiley & Sons, Inc., New York 1998

[Dz90] Dzombak, D.A., F.M.M. Morel: Surface Complexation modeling; Hydrous Ferric Oxide, Wiley-Interscience, New York, 1990

[Fe90] Fellenberg, G.: Chemie der Umweltbelastung, B.G. Teubner Stuttgart 1990

[Gr94] Gray, W.J., S.A. Steward, J.C. Tait, D.W. Shoesmith, in High Level Radioactive Waste Managment, Proceedings of the Fifth Int. Conference, American Nuclear Society 1994, pp. 2597-2601.

[Hö96] Hölting, B.: Hydrogeologie – Einführung in die Allgemeine und Angewandte Hydrogeologie, Ferdinand Enke Verlag Stuttgart 1996

[HWS56] Handbook of Chemistry and Physics 37. edition, Hodgman, Ch.D., R.C. Weast, S.M. Selby (eds): Chemical Rubber Publishing company, CO Cleveland Ohio (1955-1956)

[Ka98] Kalka, H., H. Märten, J. Hagen, R. Münze: Geochemical Infiltration Model for the Simulation of Reactive Transport in Mining Dump Sites, in Proceed. of the Intern. Workshop „Uranium Mining and Hydrogeology II“, Freiberg, September 1998, Verlag Sven von Loga, Köln 1998, 470 – 479.

[Kp00] Kashparov, A., V.P. Protsak, N. Ahamdach, D. Stammose, J.M. Peres, V.I. Yoschenko, S.I. Zvarich: Dissolution kinetics of particles of irradiated Chernobyl nuclear fuel: influence of pH and oxidation state on the release of radionuclides in the contaminated soil of Chernobyl, Journal of Nucl. Materials 279 (2000) 225-233.

[Ku98] Kulik, D.A., V.A. Sinitsyn, I.K. Karpov: Prediction of solid-aqueous equilibria in cementitious systems using Gibbs energy minimization: II. Dual thermodynamic approach to estimation of the and end-member parameters, Mat. Res. Soc. Symp. Proc. Vol. 506 (1998) 983.

[La85] Langmuir, D. and A. Riese: The thermodynamic properties of radium, Geochim. Cosmochim. Acta 49 (1985) 1593-1601.

[LS86]] Luckner, L. und W.M. Schestakow: Migrationsprozesse im Boden- und Grundwasserbereich, Deutscher Verlag für Grundstoffindustrie, Leipzig 1968

[Ma90] Matthess, G.: Die Beschaffenheit des Grundwassers, Lehrbuch der Hydrologie, Band 2, Gebrüder Borntraeger, Berlin – Stuttgart, 1990.

[Me71] Merritt, R.C.: The Extractive Metallurgy of Uranium, Colorado School of Mines Research Institute, 1971

[MH93] Morel F.M.M., J.G. Hering: Principles and Applications of Aquatic Chemistry, John Wiley & Sons, New York 1993.

[Mo95] Morrison, S.J., R.R. Spangler, V.S. Tripathi: Adsorption of amorphous ferric oxyhydroxide at high concentration of dissolved carbon(IV) and sulfur(VI), J. Contamin. Hydrology 17 (1995) 333-346

[PA99] Parkhurst, David L, Appelo, C.A.J.: User’s guide to PhreeqC (version 2) – a computer program for speciation, batch-reaction, one-dimensional transport, and inverse geochemical calculations, Water-Resources Investigation Report 99-4259, Denver, Colorado 1999

[Par95] Parkhurst, David L.: Water-Resources Investigations Report 95-4227. Lakewood, Colorado 1995.

[Pau98] Paul, M., H.J. Sänger, S. Snagowski, H. Märten, M. Eckart: Prediction of the Flooding Process at the Ronneburg Site – Results of an Integrated Approach, in Proceed. of the Intern. Workshop „Uranium Mining and Hydrogeology II“, Freiberg, September 1998, Verlag Sven von Loga, Köln 1998, 130 – 139.

[SG94] Sandino, M.C.A., B. Grambow: Solubility equilibria in the U(VI)-Ca-K-Cl-H_2O system – Transformation of schoepite into becquerelite and compreignacite, Mat. Res. Soc. Symp. Proc. Vol. 465 (1997) 1327.

[Si96] Sigg L., W. Stumm: Aquatische Chemie, vdf Hochschulverlag, Zürich 1996

[Sich94] Sich A.R.: The Chernobyl Accident Revisited: Source Term Analysis and Reconstruction of Events during the Active Phase, Massachusetts Institute of Technology, Cam-

bridge, MA 1994.

[Sin97] Sinitsyn, V.A., D.A. Kulik, M.S. Khodorivski, V.A. Kurepin, A.Y. Abramis, I.L. Kolyabina, N.A.Shurpach: Stability of mineral matter in aqueous media of the Chernobyl unit-4 shelter: thermodynamic evaluation, Mat. Res. Soc. Symp. Proc. Vol. 465 (1997) 1327.

[Sin98] Sinitsyn, V.A., D.A. Kulik, M.S. Khodorivsky, I.K. Karpov: Prediction of solid-aqueous equilibria in cementitious systems using Gibbs energy minimization: I. Multiphase aqueous – ideal solid solution models, Mat. Res. Soc. Symp. Proc. Vol. 506 (1998) 953.

[St94] Stroustrup, B.: Die C++ Programmiersprache, Addison-Wesley, Bonn 1994

[T10] Task 10: Dust Management – Dust Report, TN/00105, Slavutych, UA, April 2000.

[T13] Task 13: Shelter Water Managment – Water Characterisation and Analysis Report, TN/00139, Slavutych, UA, April 2000.

[T14R] Selected Review of Models, report T14-R10, Chernobyl NPP, Unit 4 SIP EBP Package D “Fuel Containing Materials”, Slavutych, UA, August 1999.

[T14D] Phase 1 FCM Characterisation Plan, report T14-D1, Chernobyl NPP, Unit 4 SIP EPB, Package D “Fuel Containing Materials”, Slavutych, UA, March 2000.

[UIT00] Reclamation Concept for the Schwartzwalder Mine, Golden, Colorado; Report to Cotter Corporation Lakewood, Colorado; submitted by Umwelt- und Ingenieurtechnik GmbH, Dresden, April 2000.

[Vo90] Voigt, H.-J.: Hydrogeochemie, Springer-Verlag Berlin Heidelberg New York, 1990.